

ASD TR 82-5019

AD A120272

LABORATORY SIMULATION TESTS AND INFRARED
THERMOGRAPHY OF A-10 MAIN LANDING GEAR TIRES

20000731240

ROBERT K. KIMINECZ

SEPTEMBER 1982

TECHNICAL REPORT ASD-TR-82-5019

FINAL REPORT FOR THE PERIOD JULY 1980 - DECEMBER 1981

Approved for public release; distribution unlimited.

DEPUTY FOR ENGINEERING
AERONAUTICAL SYSTEMS DIVISION
AIR FORCE SYSTEMS COMMAND
WRIGHT-PATTERSON AIR FORCE BASE, OHIO 45433

DTIC
ELECTE
OCT 13 1982

Reproduced From
Best Available Copy

82 10 12 248

DTIC FILE COPY

NOTICE

When Government drawings, specifications, or other data are used for any purpose other than in connection with a definitely related Government procurement operation, the United States Government thereby incurs no responsibility nor any obligation whatsoever; and the fact that the Government may have formulated, furnished, or in any way supplied the said drawings, specifications, or other data, is not to be regarded by implication or otherwise as in any manner licensing the holder or any other person or corporation, or conveying any rights or permission to manufacture, use, or sell any patented invention that may in any way be related thereto.

This report has been reviewed by the Office of Public Affairs (ASD/PA) and is releasable to the National Technical Information Service (NTIS). At NTIS, it will be available to the general public, including foreign nations.

This technical report has been reviewed and is approved for publication.

Robert K. Kiminecz

ROBERT K. KIMINECZ
Project Engineer
Mechanical Branch

Reuben W. Wasserman

REUBEN W. WASSERMAN
Chief, Mechanical Branch
Flight Equipment Division

FOR THE COMMANDER

Peter J. Butkewicz

PETER J. BUTKEWICZ, COL, USAF
Director
Flight Systems Engineering

If your address has changed, if you wish to be removed from our mailing list, or if the addressee is no longer employed by your organization, please notify ASD/ENFEM, WPAFB, OH 45433 to help us maintain a current mailing list.

Copies of this report should not be returned unless return is required by security considerations, contractual obligations, or notice on a special document.

Unclassified

SECURITY CLASSIFICATION OF THIS PAGE (When Data Entered)

REPORT DOCUMENTATION PAGE		READ INSTRUCTIONS BEFORE COMPLETING FORM
1. REPORT NUMBER ASD-TR-82-5019	2. GOVT ACCESSION NO. AD-A120272	3. RECIPIENT'S CATALOG NUMBER
4. TITLE (and Subtitle) LABORATORY SIMULATION TESTS AND INFRARED THERMOGRAPHY OF A-10 MAIN LANDING GEAR TIRES		5. TYPE OF REPORT & PERIOD COVERED Final Report July 1980 - December 1981
		6. PERFORMING ORG. REPORT NUMBER
7. AUTHOR(s) Robert K. Kiminecz		8. CONTRACT OR GRANT NUMBER(s)
9. PERFORMING ORGANIZATION NAME AND ADDRESS Deputy for Engineering Aeronautical Systems Division Wright-Patterson Air Force Base, Ohio 45433		10. PROGRAM ELEMENT, PROJECT, TASK AREA & WORK UNIT NUMBERS Program Element 27131F Project 64329A
11. CONTROLLING OFFICE NAME AND ADDRESS OO-ALC/MMI Hill AFB, UT 88406		12. REPORT DATE September 1982
		13. NUMBER OF PAGES 83
14. MONITORING AGENCY NAME & ADDRESS (if different from Controlling Office)		15. SECURITY CLASS. (of this report) Unclassified
		15a. DECLASSIFICATION/DOWNGRADING SCHEDULE
16. DISTRIBUTION STATEMENT (of this Report) Approved for public release; distribution unlimited.		
17. DISTRIBUTION STATEMENT (of the abstract entered in Block 20, if different from Report)		
18. SUPPLEMENTARY NOTES		
19. KEY WORDS (Continue on reverse side if necessary and identify by block number) Aircraft Ground Loads Landing/Taxi Simulation Aircraft Tires Taxi/Takeoff Simulation A-10 Tires Tire Infrared Thermography		
20. ABSTRACT (Continue on reverse side if necessary and identify by block number) This report describes the test procedures and results that were used in evaluating the A-10 main landing gear tires. Continued on Reverse		

DD FORM 1 JAN 73 1473

EDITION OF 1 NOV 65 IS OBSOLETE

Unclassified

SECURITY CLASSIFICATION OF THIS PAGE (When Data Entered)

Block 20 Continued.

Infrared thermography was used to measure tire surface temperatures during aircraft taxi tests and laboratory tests. Since the A-10 operates with a toe-out alignment of the main gear, particular emphasis was placed on the determination of the effect of small slip angles on tire surface temperature distribution. Preliminary laboratory tests were conducted to obtain small slip angle carpet plots while simultaneously measuring the tire surface temperature. The results of these tests showed that operating a tire with small positive slip angles resulted in consistently higher outboard (versus inboard) sidewall temperatures. The magnitude of the difference between sidewall surface temperatures (outboard minus inboard) appeared to be a linear function of small slip angles. The tires were then rolled to failure with a fixed one degree slip angle to determine the surface temperature distribution at or near tire failure.

A laboratory test plan that simulated A-10 operations at Myrtle Beach AFB was written as a series of dynamics statements that were used to program a computer controlled tire test dynamometer. These tests dynamically simulated all loads, velocities, turns, stops and distances rolled by an A-10 main landing gear tire from the time the aircraft leaves the chocks until it is airborne and from the time it lands until it returns to the chocks. The simulation tests resulted in laboratory tire failures that were in agreement with field failure data for the small sample of tires that were tested.

FOREWORD

The work presented herein was performed in support of the A-10 Systems Program Office (SPO) at Wright-Patterson Air Force Base during the time period from July 1980 to December 1981. The Program Element Number was 27131F, and the Project Number was 64329A.

The author wishes to acknowledge the significant contributions to this effort that were made by the following:

Bill Stowe, A-10 SPO Engineering, whose continuing interest and suggestions kept the project moving forward.

Harry Schmidt, formerly of the A-10 SPO, who initiated the taxi tests and compiled the early tire failure data.

Tony Levan of Systems Research Laboratories who programmed the computer controlled dynamometer for the simulation tests.

John Barbagallo, 6520TG/ENAS at Edwards AFB, who obtained the ambient, airfield, and tire pyrometer readings during the taxi tests.

John Hermayer of the Fairchild Republic Company for his help in the instrumentation during the taxi tests.

Bob Bent, Tom Stahl, and Bill Maggard of Systems Research Laboratories for obtaining the thermography data during the laboratory testing.

Charlotte Spieth, Gloria Walker, and Mary Huttzell for their assistance in the preparation of this report.

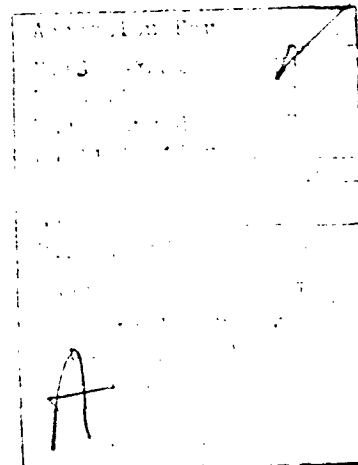


TABLE OF CONTENTS

SECTION PAGE

I	INTRODUCTION	1
	1. Background	1
	2. Objective of Testing	2
II	TIRE FIELD DATA	3
	1. Tire Identification	3
	2. Tire Failure Data	3
	3. Tire Wear Data	5
III	TIRE TEMPERATURES	7
	1. Introduction	7
	2. Tire Infrared Thermography	8
IV	TESTING	12
	1. Preliminary Laboratory Tests	12
	a. Roll to Failure Tests	12
	b. Surface Temperature Versus Slip Angle Tests	19
	2. Aircraft Taxi Tests	19
	3. Myrtle Beach Simulation Laboratory Test	24
	a. Approach	26
	b. Taxi-Takeoff Simulations	28
	c. Landing-Taxi Simulations	45
	d. Simulation with 0 Degree Toe-Out	45
	e. Tire Failures During the Simulation Tests	45
V	CORRELATION OF RESULTS	53
	1. Average Tire Surface Temperatures	53
	2. Effect of Slip Angle on Tire Surface Temperature	62
	3. Other Influences on Tire Surface Temperature	
	a. Ambient, Runway and Flywheel Temperatures	64
	b. Speed	64
	c. Circumferential Temperature Variation	65

TABLE OF CONTENTS (CONT'D)

VI	CONCLUSIONS	66
VII	RECOMMENDATIONS	67
APPENDICES		
A	CORNERING FORCE CARPET PLOT FOR TIRES A, B, AND C	68
B	DETAILED DYNAMICS STATEMENTS FOR THE MYRTLE BEACH SIMULATION	70
C	CONTAINED AIR TEMPERATURE AND PRESSURE DURING THE SIMULATION TESTS	81
REFERENCES		83
BIBLIOGRAPHY		83

LIST OF ILLUSTRATIONS

FIGURE		PAGE
1.	Tire and Front-Surfaced Mirrors for the Simultaneous Measurement of Tread and Sidewall Surface Temperatures	9
2.	Development of Thermograph with Front-Surfaced Mirrors and Nomenclature of Significant Temperature Peaks and Valleys	11
3.	Rise in Surface and Contained Air Temperature During the Roll to Failure Test of Tire A	13
4.	Rise in Surface and Contained Air Temperature During the Roll to Failure Test of Tire B	14
5.	Rise in Surface and Contained Air Temperature During the Roll to Failure Test of Tire C	15
6.	Peak Sidewall Temperature Difference as a Function of Slip Angle, Normal Load and Inflation Pressure at a Constant Flywheel Speed of 46 MPH for Tire A	17
7.	Peak Sidewall Temperature Difference as a Function of Slip Angle, Normal Load and Inflation Pressure at a Constant Flywheel Speed of 46 MPH for Tire B	18
8.	Peak Sidewall Temperature Difference as a Function of Slip Angle, Normal Load and Inflation Pressure at a Constant Flywheel Speed of 46 MPH for Tire C	19
9.	Taxi Test Procedure	21
10.	Taxi Test Tire Surface Temperature Rise at 0° Toe-Out	22
11.	Taxi Test Tire Surface Temperature Rise with 0.8° and 1.4° Toe-Out	23
12.	Taxi-Takeoff Conditions used in the Myrtle Beach Simulation	27
13.	Comparison of Tire Surface Temperatures During the Long Distance Taxi-Takeoff Simulation	
	a. Stopped for Arming	29
	b. Stop before Takeoff	30
	c. Airborne	31
14.	Comparison of Tire Surface Temperature Rise During the Short Distance Taxi-Takeoff Simulation	
	a. Stopped for Arming	32
	b. Stop before Takeoff	33
	c. Airborne	34

LIST OF ILLUSTRATIONS (CONT'D)

FIGURE

15.	Comparison of Tire Surface Temperature Rise During the Heavy Gross Weight Long Distance Taxi-Takeoff Simulation	
a.	Stopped for Arming	35
b.	Stop before Takeoff	36
c.	Airborne	37
16.	Landing-Taxi Conditions used in the Myrtle Beach Simulation	38
17.	Comparison of Tire Surface Temperature Rise During the Landing-Long Distance Taxi Simulation	
a.	After Landing Roll	39
b.	Stop for Dearing	40
c.	Parked	41
18.	Comparison of Tire Surface Temperature Rise During the Landing-Short Distance Taxi Simulation	
a.	After Landing Roll	42
b.	Stop for Dearing	43
c.	Parked	44
19.	Comparison of Tire B Surface Temperatures with 0.8° and 0° Toe-Out During the Long Distance Taxi-Takeoff Simulation	46
20.	Comparison of Tire B Surface Temperatures with 0.8° and 0° Toe-Out During the Short Distance Taxi-Takeoff Simulation	47
21.	Comparison of Tire B Surface Temperature with 0.8° and 0° Toe-Out During the Heavy Gross Weight Long Distance Taxi-Takeoff Simulation	48
22.	Comparison of Tire B Surface Temperature with 0.8° and 0° Toe-Out During the Landing-Long Distance Taxi Simulation	49
23.	Comparison of Tire B Surface Temperatures with 0.8° and 0° Toe-out During the Landing-Short Distance Taxi Simulation	50
24.	Average Tire Surface Temperature Rise Versus Applied Load Times Accumulated Distance for Laboratory Roll to Failure and Simulation Tests of Tire A	58
25.	Average Tire Surface Temperature Rise Versus Applied Load Times Accumulated Distance for Laboratory Roll to Failure and Simulation Tests of Tire B	59
26.	Average Tire Surface Temperature Rise Versus Applied Load Times Accumulated Distance for Laboratory Roll to Failure and Simulation Tests of Tire C	60

LIST OF ILLUSTRATIONS (CONT'D)

FIGURE		PAGE
27.	Average Tire Surface Temperature Rise Versus Applied Load Times Accumulated Distance Comparison Between Laboratory Roll to Failure Test and Taxi Tests for Tire A	61
28.	Average Tire Surface Temperature Rise per Elapsed Test Time Versus Applied Load Times Accumulated Distance for Laboratory Roll to Failure and Simulation Tests of Tire A	63
A-1.	Cornering Force Carpet Plot at Small Slip Angles	69

LIST OF TABLES

TABLE	PAGE
1. A-10 Main Tire Failures - Aug 1979 to Aug 1981	3
2. Tire Inventory from A-10 Field Units - May 1981	4
3. Comparison of Tire Failures One Year Before and One Year After the Change to Two Inflation Pressures	5
4. Tread Depth Measurements at Myrtle Beach AFB - July 1981	6
5. Taxi Test Conditions	20
6. Myrtle Beach Simulation Test Conditions	25
7. Tire Performance During the Myrtle Beach Simulation Tests	51
3. Average Tire Surface Temperature Rise During Laboratory and Field Testing	54
C-1. Contained Air Temperature and Pressure for Laboratory Simulation Tests	82

SECTION I

INTRODUCTION

1. BACKGROUND

One of the concepts in the A-10 procurement was the preferential use of off-the-shelf components. Two main landing gear tires were available which met or exceeded the A-10 requirements: the 36 x 11/22 PR tire used on the C-141 nose gear and the 36 x 11/24 PR tire used on the F-105 main gear. Since the 22 PR tire was retreadable and the 24 PR tire was not, the 22 PR tire was chosen for life cycle cost considerations. The main landing gear wheel was then designed and qualified using the 22 PR tire.

In 1976, the A-10 began experiencing damaging 22 PR tire failures which prompted a decision to switch to the 24 PR tire. The 24 PR tire gave excellent service on the aircraft with only one known failure in two years. But in 1978 main wheel failures began and laboratory testing showed that the 24 PR tire imposed a much higher stress on the wheel and was therefore contributing to premature wheel failure. In 1980, the decision was made to purge the fleet of 24 PR tires and return to the exclusive use of 22 PR tires. Tire failures reoccurred and the A-10 Systems Program Office at Wright-Patterson Air Force Base was confronted with the task of eliminating these failures. The following actions were taken to reduce 22 PR tire failures:

(1) A change from seven to two inflation pressures. The original specification called for seven different tire pressures dependent upon aircraft gross weight. This was changed to an inflation pressure of 155 psi for aircraft gross weights of 40,000 lbs and below and 185 psi for gross weights above 40,000 lbs. The rationale for this action was that the tire with 155 psi inflation, which applies to 98% of present A-10 operating gross weights, would be operating with deflections of 32% or less, and as is well known in the tire industry these lower deflections will reduce the chances of dynamic tire failure. Also, the change from seven to two tire pressures would make it less of a maintenance problem in the field and thus reduce the chances of inadvertently operating with an overdeflected tire.

(2) Requirement for Holographic Inspection of Recapped Tires. This requirement was instituted in late 1980 with the intent of preventing tires with ply separations or other defects from being recapped and sent back to the fleet.

While these two actions led to a significant reduction in aircraft damaging tire failures, the failure rate remained unacceptably high and long term corrective actions including laboratory and field testing were initiated.

2. OBJECTIVE OF TEST PROGRAM

The objective of the tire test program was to determine whether the toe-out alignment of the main landing gear significantly decreases the fatigue life of the tires or contributes to premature tire failure. While it is well known that continuous operation of a tire under a yawed condition will accelerate tire wear, it is not known to what extent this decreases the fatigue life of the tire carcass or contributes to failure due to tread separation. Laboratory and field test plans were written with the objective of determining the effect of wheel alignment on tire surface temperature and to correlate (if possible) any increased tire temperature due to misalignment with uneven tread wear and premature tire failure. The tires that were tested included the currently used 22 PR tires of two different manufacturers and the 24 PR tire.

SECTION II

TIRE FIELD DATA

1. TIRE IDENTIFICATION

This report was concerned with the laboratory and field performance of three different tires. Throughout this report, these tires will be designed as follows:

Tire A is a 36 x 11/22 PR tire currently used on the A-10.

Tire B is a 36 x 11/22 PR tire currently used on the A-10 but from a different manufacturer than Tire A.

Tire C is a 36 x 11/24 PR tire that saw interim use on the A-10 but was removed because of main wheel failures.

Tires A and B were originally qualified for the C-141 nose; Tire C was qualified for the F-105 main. All three tires have given excellent service on their respective aircraft.

2. TIRE FAILURE DATA

The number of reported failures in the time period from August 1979 to August 1981 are shown in Table 1.

TABLE 1
A-10 MAIN TIRE FAILURES
AUG 1979 to AUG 1981

<u>TIRE I.D.</u>	<u>NUMBER OF FAILURES</u>	<u>PERCENT OF TOTAL</u>
A	17	25
B	1	1
A-RETREAD	26	38
B-RETREAD	2	3
UNKNOWN	23	33
TOTAL	69	100

Of the 69 total failures, 20 were reported to have caused aircraft damage.

While Table 1 suggests that most of the tire failures occurred with Tire A (new and retread), it was not known at what relative quantities tires A and B were being supplied to the field. In April 1981 a message was sent to A-10 field units requesting a tire inventory. Their response is shown in Table 2.

TABLE 2
TIRE INVENTORY FROM
A-10 FIELD UNITS - MAY 1981

<u>TIRE I.D.</u>	<u>NUMBER REPORTED</u>	<u>PERCENT OF TOTAL</u>
A	308	54
B	139	24
A-RETREAD	72	13
B-RETREAD	49	9
TOTAL . . .	568	100

These data from Table 2 were for tires on the aircraft as well as tires in base supply. While Table 2 cannot be directly correlated with Table 1 because of the time spans involved, it does show a sufficient quantity of Tire B in the field.

As stated earlier, the interim change from seven to two tire pressures and the holographic inspection of retreads led to a significant reduction in tire failures. A summary of number and type of failures before and after the inflation pressure change is shown in Table 3.

TABLE 3
COMPARISON OF TIRE FAILURES
ONE YEAR BEFORE AND ONE YEAR
AFTER THE CHANGE TO TWO
INFLATION PRESSURES

<u>FAILURE MODE</u>	<u>NUMBER OF FAILURES</u>	
	<u>AUG 79 TO AUG 80</u>	<u>AUG 80 TO AUG 81</u>
Tread Separation	18	5
Sidewall Failure	13	5
Air Leak	8	14
Unknown	3	3
Total . . .	42	27

The number of failures that resulted in aircraft damage were 15 before and 5 after the change to two tire pressures.

3. TIRE WEAR DATA

The toe-out alignment of the main gear causes the inboard part of the tread to wear at a faster rate than the outboard part of the tread. This asymmetric tread wear was reported early in the program by A-10 maintenance personnel. To better quantify the uneven tread wear, tread depth measurements were taken on tires in various states of wear at Myrtle Beach AFB in July 1981. These results were averaged and are shown in Table 4.

TABLE 4
TREAD DEPTH MEASUREMENTS AT
MYRTLE BEACH AFB - JULY 1981

		<u>TREAD GROOVE DEPTH IN INCHES</u>			
<u>TIRE</u> <u>I.D.</u>	<u>STATE</u>		CENTER	CENTER	
		<u>OUTBOARD</u>	<u>OUTBOARD</u>	<u>INBOARD</u>	<u>INBOARD</u>
A	New	0.44	0.44	0.44	0.44
A	Worn*	0.37	0.32	0.29	0.26
A	Worn Out**	0.28	0.19	0.10	0.0
B	New	0.28	0.41	0.41	0.28
B	Worn***	0.23	0.32	0.31	0.15
B	Worn Out****	0.16	0.22	0.20	0.0

* Average of 34 tires on aircraft

** Average of 4 tires in shop

*** Average of 12 tires on aircraft

**** Average of 2 tires in shop

SECTION III

TIRE TEMPERATURES

1. INTRODUCTION

A rolling tire generates heat by the cyclic deformation of tread and carcass and the hysteresis losses of the materials. As the tire temperature increases: the rate of tread wear increases, the coefficient of friction decreases, and fatigue resistance of the carcass is reduced. If the tire operating temperature is in the range from 250 to 300°F, then some form of heat damage is generally conceded. At 350°F and above, heat damage of the standard aircraft tire is a certainty and failure is probable. Incipient failure may begin by fatigue initiation at a flaw and progress due to an increase in the local temperature which further reduces the fatigue resistance; so that the mechanism of tire failure is usually attributed to the combined effects of temperature and fatigue.

An automobile or truck tire is designed for continuous operation and will reach an equilibrium temperature where the rate of heat generation equals the rate of heat dissipation. Aircraft tires are designed for intermittent operation only - taxi takeoffs and landing taxis with relatively long periods of time between operations which permit tire cooling. If subjected to a continuous roll at rated load and inflation pressure at a typical taxi speed, the standard aircraft tire would not achieve temperature equilibrium but would sustain an increasing temperature rise until failure occurred - typically, within 30 miles from start of roll.

The measurement of internal carcass and tread temperatures of rolling aircraft tires presents a difficult problem. Thermocouples have been layed in the uncured tire during buildup, or holes have been drilled in the cured tire and the thermocouples inserted and cemented in place. In either case, when the tire is loaded and rolled, the sensors tend to fail prematurely, particularly in regions of high flexure. Even when successful, the embedded sensor represents an inhomogeneity in the region of measurement and could create a hot spot and provide questionable data. The thermocouple material most commonly used for this application is copper-constantan which is available in small gauge and fine

stranded wire which is more durable than solid wire. An alternative method for measuring internal tire temperature is to roll the tire a predetermined distance, stop the roll, and probe the tire body with a thermocouple needle. This method requires considerable testing to obtain a thorough mapping of temperature rise and, when testing high pressure aircraft tires, the tire is often deflated before probing as a safety precaution.

Contained air temperature is routinely measured using thermocouples, thermistors, or diodes in conjunction with either slip rings or telemetry.

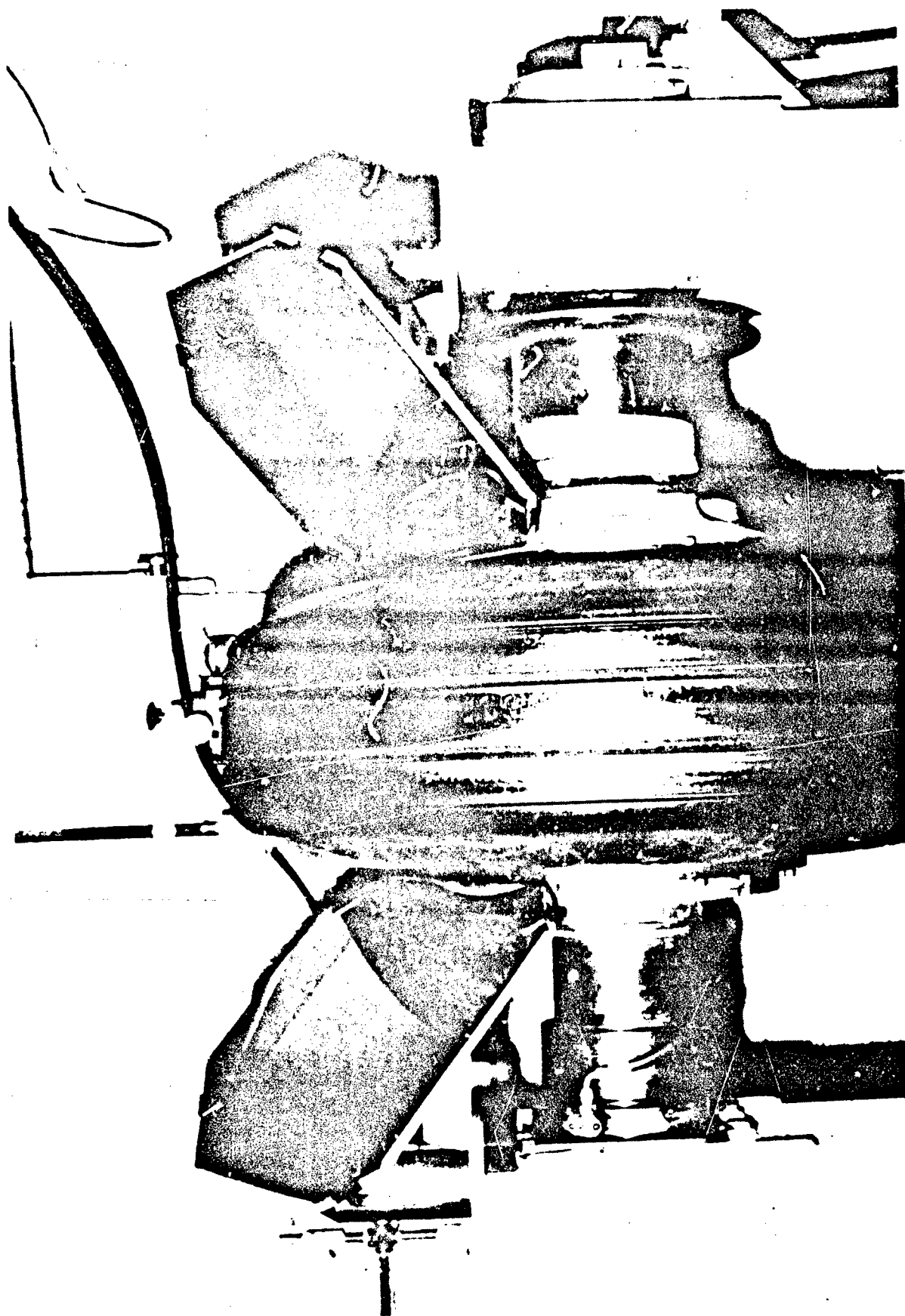
2. TIRE INFRARED THERMOGRAPHY

Infrared thermography has been used by the tire industry, primarily as a research tool, since the early 1970s. Trivisonno used surface temperature as one of the inputs to his thermal analysis to calculate steady-state tire body temperatures and power loss of radial and bias ply passenger tires (Reference 1). In 1972, Trivisonno successfully applied these methods and performed a non-steady-state analysis of a 49 x 17 aircraft tire (Reference 2). In 1970, Conant, Hall and Walter used infrared thermography measurements on radial, bias and bias-belted automobile tires that were instrumented with embedded thermocouples (Reference 3). These data were obtained at different loads, speeds and inflation pressures and input to a designed experiment to demonstrate the effects on tire surface temperature of the aforementioned operating conditions.

This report compared the surface temperature of 36 x 11 tires on an aircraft during taxi tests and during a laboratory simulation of A-10 operating conditions. Particular emphasis was placed on the effect of small slip angles on surface temperature distribution.

The infrared system used in these tests was an Inframetrics Model 525 capable of full field presentation of thermal images in either calibrated grey or colors (different temperatures show up as different colors). The line scan presents the data as a thermal profile of a horizontal line across the tire. Since it presents a somewhat more quantitative picture of tire temperature, the line scan mode was used throughout this testing.

For laboratory testing, two front surfaced mirrors were mounted on the test machine mandrel to permit the simultaneous measurement of tread and sidewall



temperatures. A mounted tire and mirror arrangement is shown in Figure 1. To minimize the chance of damage to the infrared detector in the event of a tire failure, the detector was equipped with a telescopic lens and mounted 30 feet distant from the running tire. The thermography data was recorded on video tape and voice annotated with pertinent information. The video tape was replayed and the thermal profile was Polaroid photographed, the temperatures measured and recorded.

Figure 2 shows how the thermal profile relates to the tire surface temperature. Generally, the tread ribs are the coolest part of the tire surface. The ribs are cooled by conduction to the flywheel surface and, since they are at the maximum diameter of the tire, receive the maximum convection cooling because of their higher speed through the air. The tread grooves are not cooled by conduction to the flywheel and are closer to the source of heat generation and run considerably hotter than the tread ribs.

The sidewall temperatures were usually the highest at a point above the bead corresponding to the apex region of the ply turnups. The sidewall minimum was at the minimum section approximately midway between apex and shoulder.

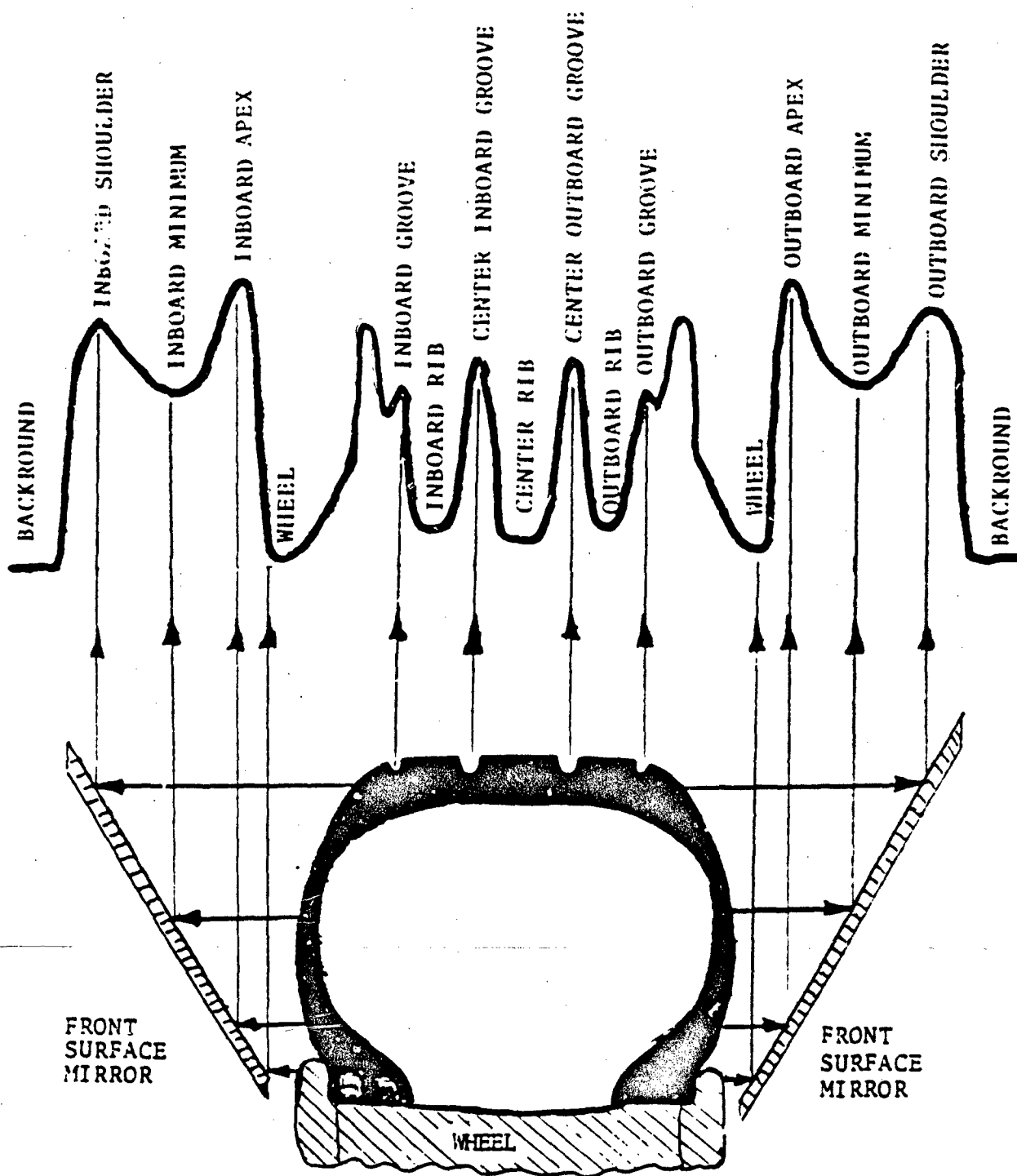


Figure 2. Development of Thermograph with Front-Surfaced Mirrors and Nomenclature of Significant Temperature Peaks and Valleys

SECTION IV

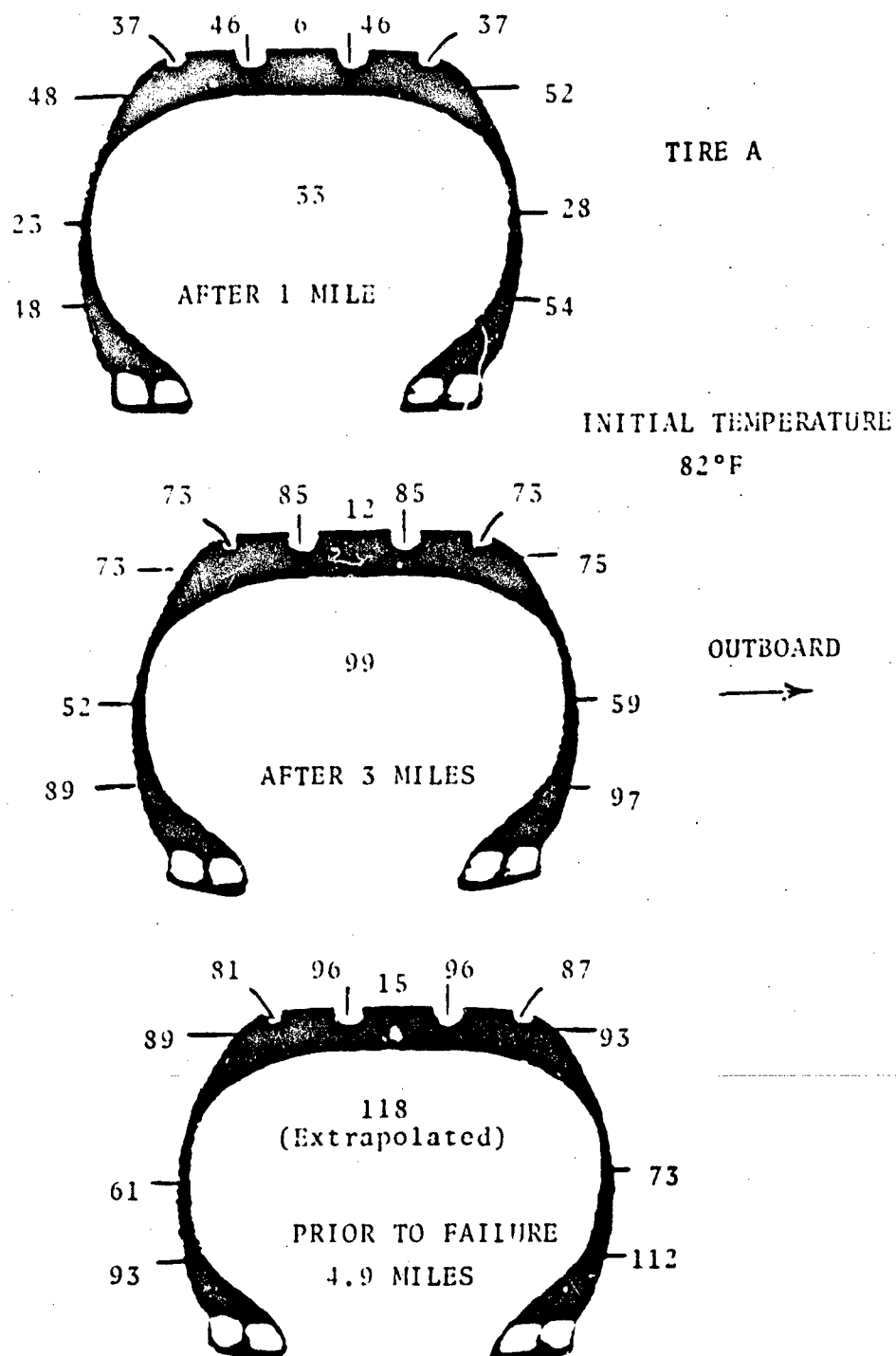
TESTING

1. PRELIMINARY LABORATORY TESTS

The objective of these tests, conducted at Wright-Patterson Air Force Base, was to develop preliminary laboratory data for comparison with field test data. Since the A-10 was known to operate with a toe-out condition of the main gear, laboratory tests were conducted emphasizing the effect of small slip angles on tire surface temperature. Carpet plots of cornering force versus normal load and slip angle were developed, and Tires A, B and C were rolled to failure to establish what surface temperatures obtain at or near tire failure. These tests were conducted on the 120 inch diameter programmable dynamometer.

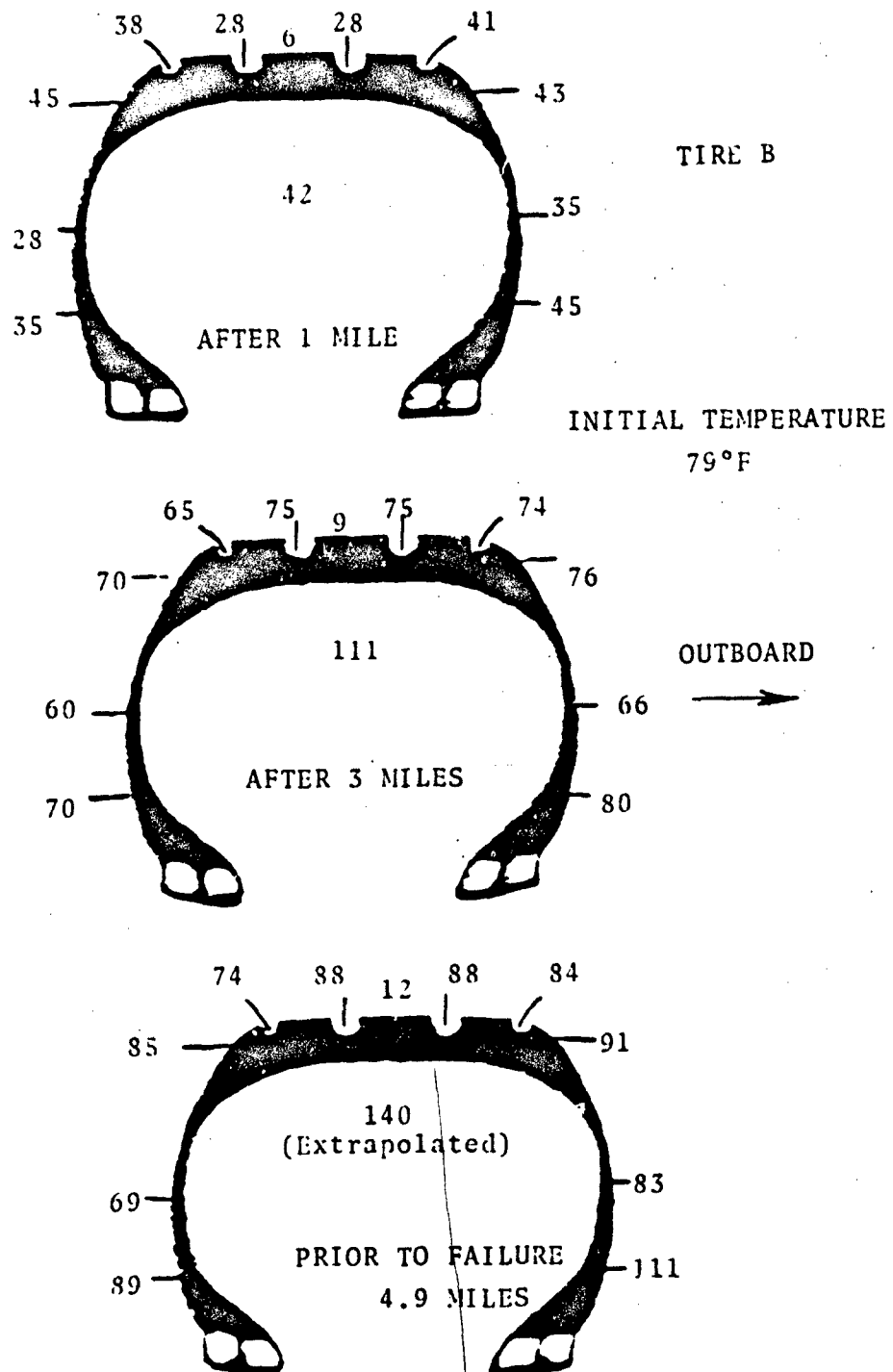
a. Roll to Failure Tests

To establish the surface temperatures that would indicate detrimental tire operation, Tires A, B and C were rolled to failure with a 1° slip angle, 20,000 pounds normal load, 150 psi inflation and at a speed of 46 mph. This speed corresponds to 40 knots which was an estimate of the unbraked A-10 ground idle speed. Figures 3, 4 and 5 show the surface and contained air temperature rise as measured at 1 mile, 3 miles and prior to failure for Tires A, B and C respectively. The surface temperature rise, rather than the surface temperature, was used throughout this report so that the tire temperatures could be more directly compared. The initial laboratory ambient temperatures, while not the same for all tests, were within a relatively narrow range. The actual surface temperatures may be obtained by adding the initial temperature to the temperature rise. The 1° slip angle which simulates main gear toe-out, causes the outboard sidewall to experience more flexure than the inboard sidewall. This additional flexure results in the outboard sidewall generating more heat than the inboard sidewall. As shown in Figures 3, 4 and 5, the outboard sidewall surface temperature rise was greater than the corresponding inboard sidewall temperature rise, and in every case, the maximum surface temperature was at the apex region of the outboard sidewall. All three tires failed by blowout of the outboard sidewall at the apex region.



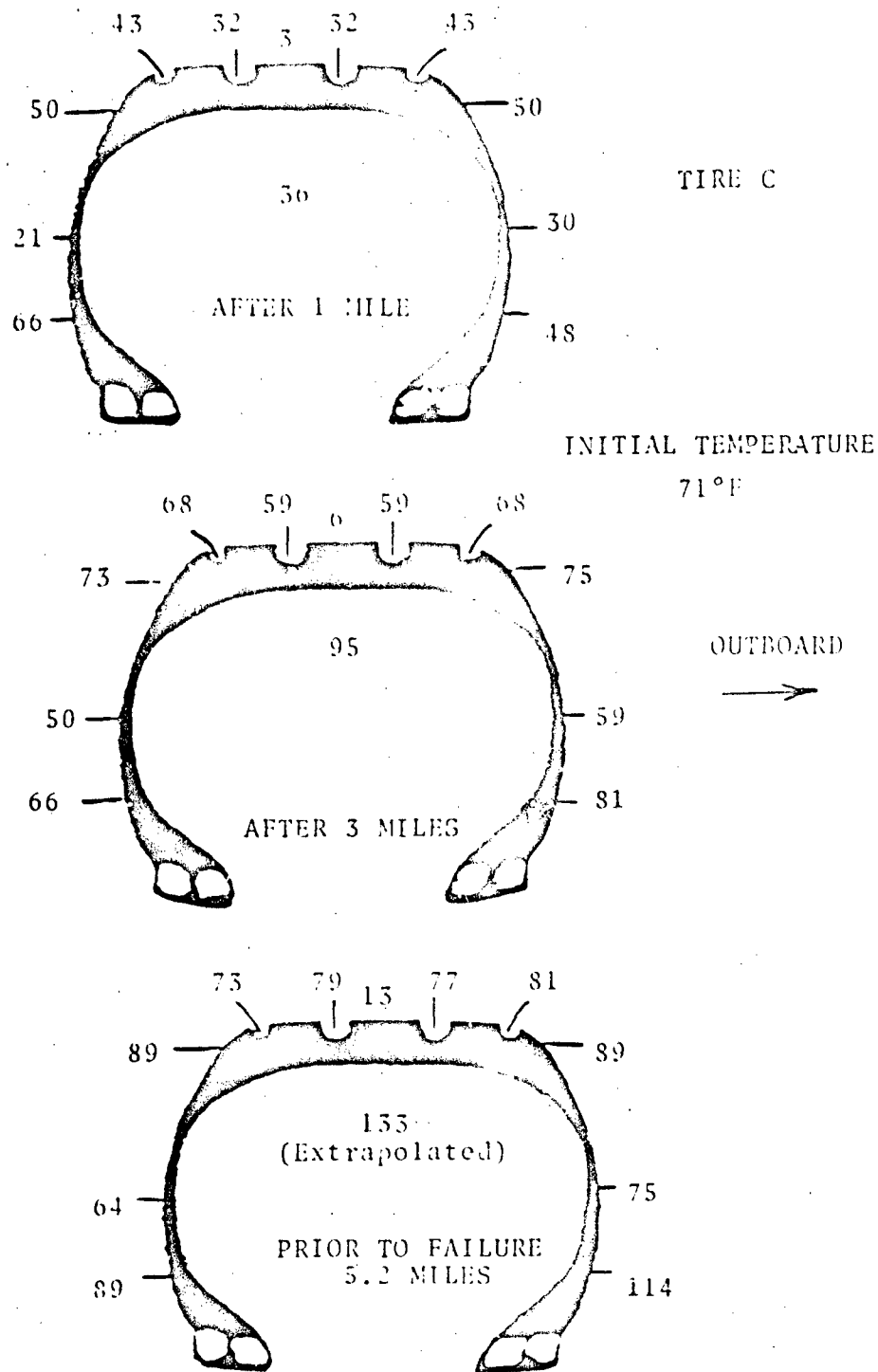
CONDITIONS: 20,000 LBS Load, 150 PSI, 46 MPH, 1° Slip Angle

Figure 3. Rise in Surface and Contained Air Temperature During the Roll to Failure Test of Tire A



CONDITIONS: 20,000 LBS Load, 150 PSI, 46 MPH, 1° Slip Angle

Figure 4. Rise in Surface and Contained Air Temperature During the Roll to Failure Test of Tire B



CONDITIONS: 20,000 LBS Load, 150 PSI, 46 MPH, 1° Slip Angle

Figure 5. Rise in Surface and Contained Air Temperature During the Roll to Failure Test of Tire C

b. Surface Temperature Versus Slip Angle Tests

Carpet plots of cornering force versus normal load and inflation pressure were developed for slip angles of 0, 0.5, 1.0 and 1.5 degrees while simultaneously taking surface temperatures. These data were taken after the tires had rolled 2 miles. Since the effect of the slip angle was to cause the outboard sidewall to run hotter than the inboard sidewall, this temperature difference (maximum outboard minus maximum inboard) was plotted for Tires A, B and C in Figures 6, 7 and 8 respectively. As shown by these plots, the peak sidewall temperature difference appears to be linear for the slip angles tested and not dependent on load and inflation. The negative temperature difference exhibited by Tires A and B at 0° slip angle was probably due to tire conicity and ply steer or test machine bias.

2. AIRCRAFT TAXI TESTS

These tests, conducted at Edwards Air Force Base, were for the purpose of obtaining thermography data under aircraft taxiing conditions. The infrared detector was installed behind the left main tire in a support which replaced the landing gear door. The detector was rigidly mounted for viewing the tire tread during the taxi run. A quick release mechanism was used to allow removal of the detector prior to a run and immediately after a run to permit scanning of the tire sidewalls. The thermography signal conditioning and recording instrumentation were operated in the battery power mode and rigidly secured inside an aircraft bay. The video tape was voice annotated by the test engineers during initial and final temperature measurements and by the test pilot during the taxi. The aircraft was tested to the conditions of Table 5. The tires on the aircraft were Tire A.

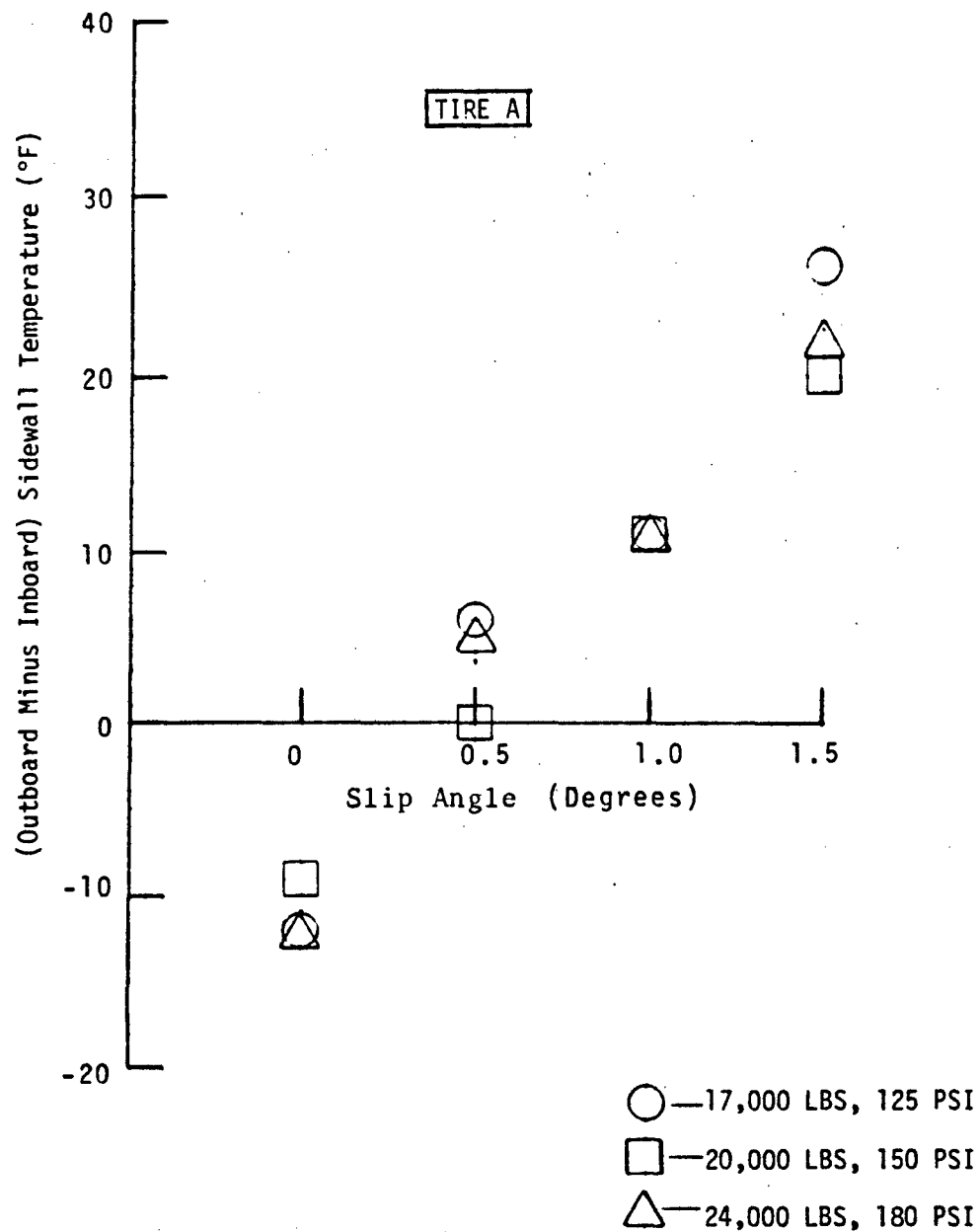


Figure 6. Peak Sidewall Temperature Difference as a Function of Slip Angle, Normal Load and Inflation Pressure at a Constant Flywheel Speed of 46 MPH

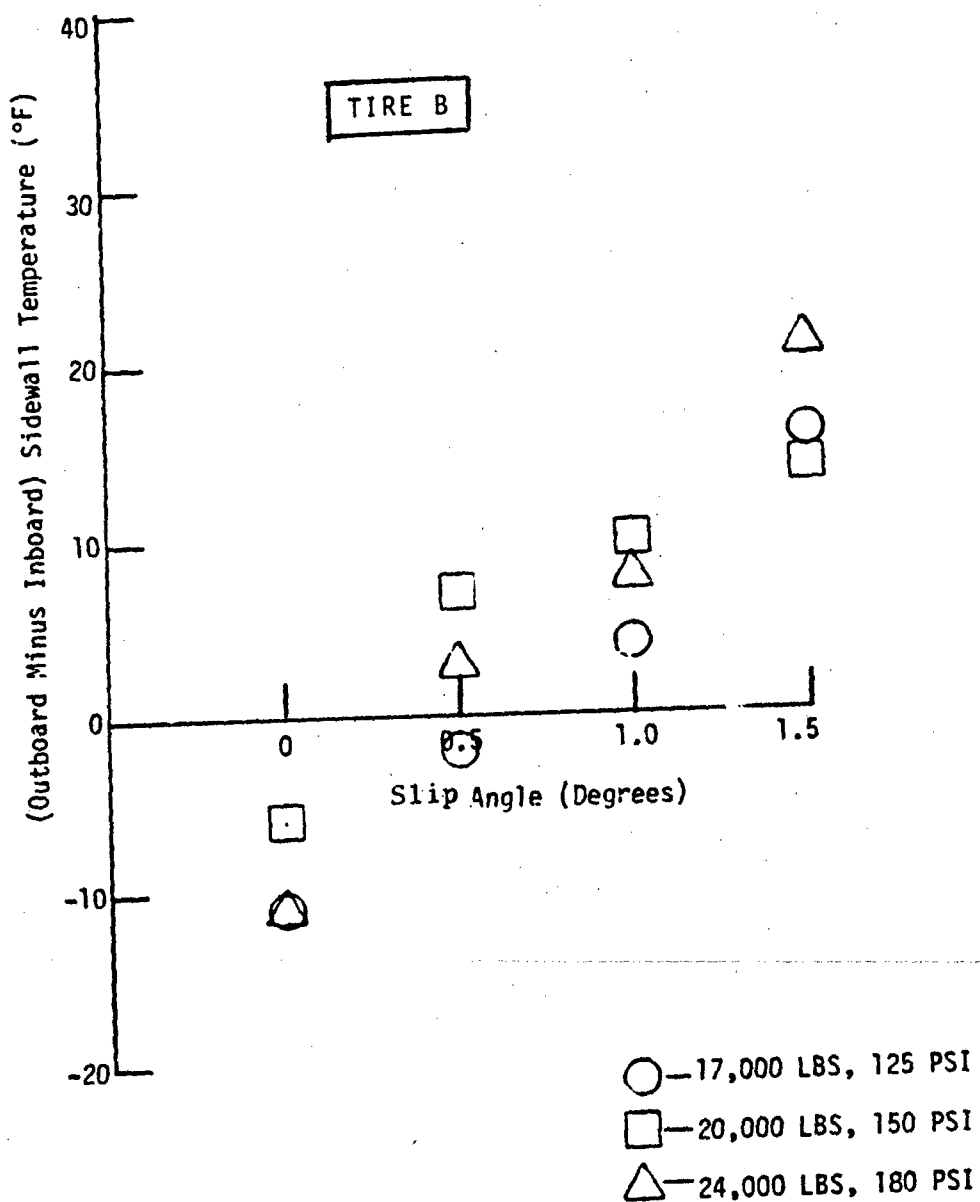


Figure 7. Peak Sidewall Temperature Difference as a Function of Slip Angle, Normal Load and Inflation Pressure at a Constant Flywheel Speed of 46 MPH

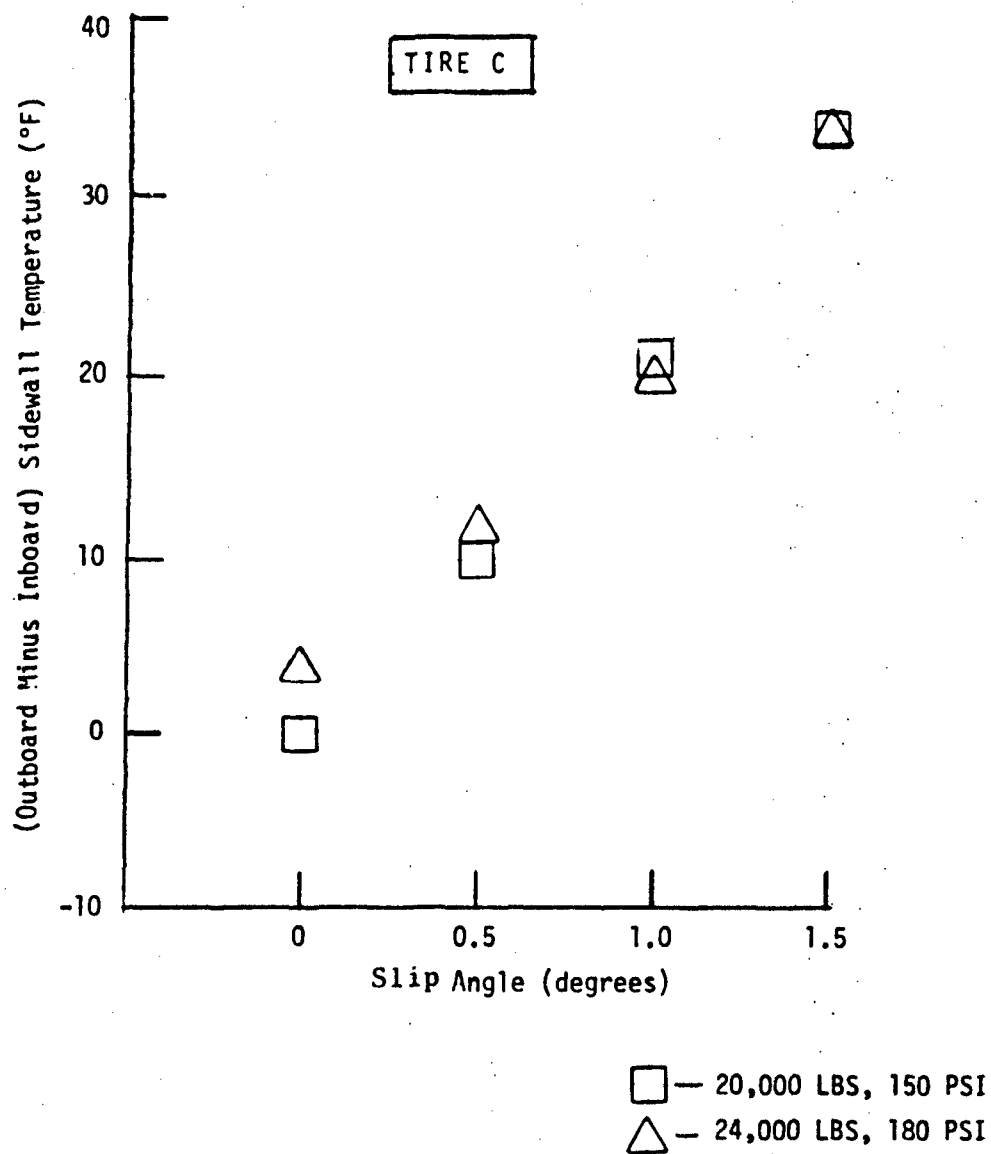


Figure 8; Peak Sidewall Temperature Difference as a Function of Slip Angle, Normal Load and Inflation Pressure at a Constant Flywheel Speed of 46 MPH

TABLE 5

TAXI TEST CONDITIONS

<u>RUNS</u>	<u>AIRCRAFT</u>	<u>TIRE</u>	<u>TOE-OUT</u>	
	<u>GROSS WEIGHT (LB)</u>	<u>INFLATION (PSI)</u>	<u>(DEGREES)</u>	<u>SPEED (KTS)</u>
1&2	34,500	125	0	40
3&4	34,500	125	0.8	40
5&6	40,000	150	0	40
7&8	40,000	150	1.4	40
9&10	48,000	180	0	40
11&12	48,000	180	1.4	40

The toe-out angles of both main gear were varied using a specially constructed torque link and measured with respect to the aircraft centerline. After the required toe-out angle was set, the aircraft was configured with the stores and fuel necessary to achieve the desired gross weight and then towed to a taxiway position that was approximately 400 feet from the test runway. Here, the aircraft was parked and the tires cooled by a refrigerated air cooler until the surface temperature, as measured with a Wahl Pyrometer, was reasonably close to ambient. To establish initial tire surface temperatures, the pyrometer was used to measure and record tread and sidewall temperatures and these temperatures were correlated with the infrared scans. Other data taken and recorded prior to taxi were ambient and runway temperatures and wind speed and direction.

After the initial data were recorded and permission to taxi given by the control tower, the tests proceeded as shown in Figure 9. Turning onto and off the runway required two right turns. During the acceleration, constant speed and deceleration, the test pilot attempted to minimize the use of nose wheel steering and braking. As soon as the aircraft stopped in the inspection area, the test engineers recorded tread and sidewall temperatures and these final temperatures were compared with the initial temperatures prior to taxi to yield tire temperature rise data. Two runs were made for each test condition of Table 5. These two runs were averaged and the resulting surface temperature profiles are shown in Figures 10 and 11.

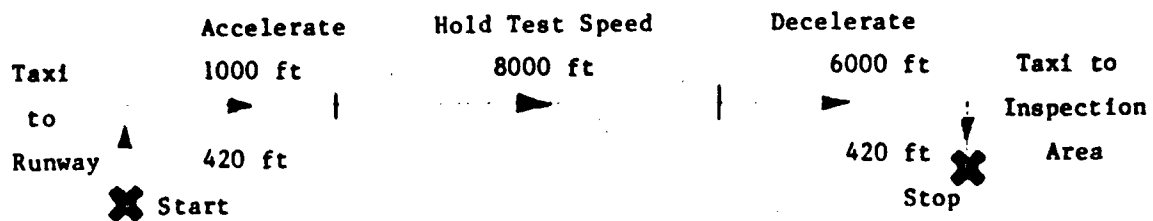
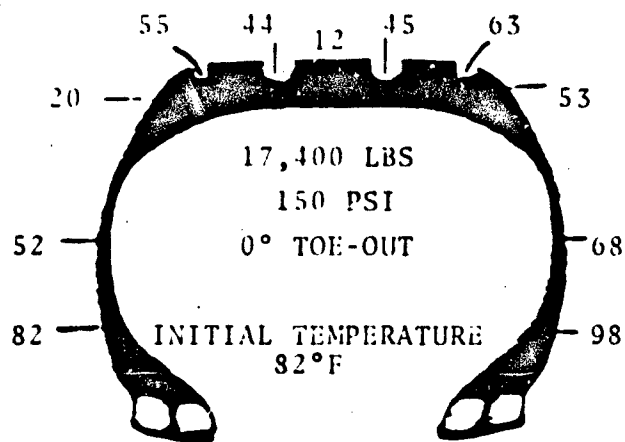
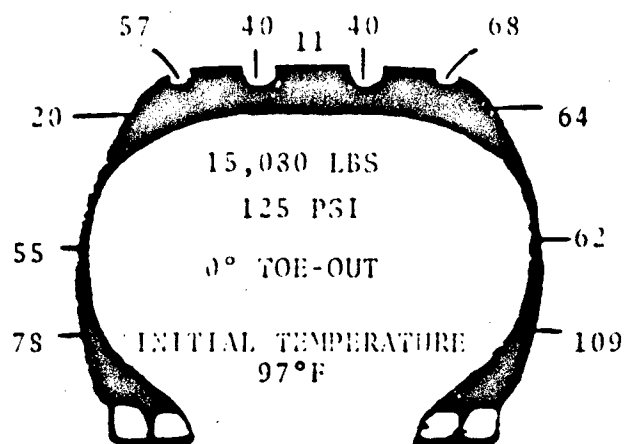


Figure 9. Taxi Test Procedure



OUTBOARD

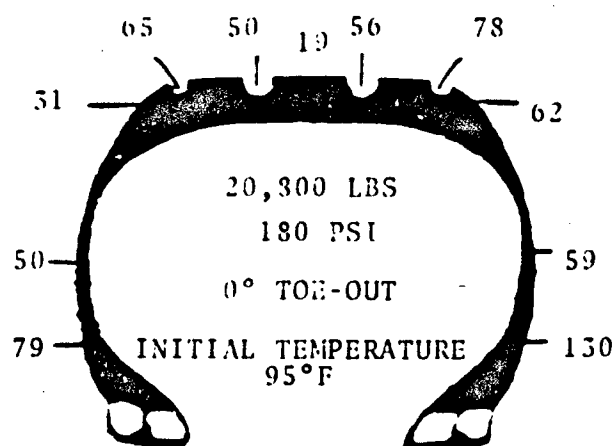
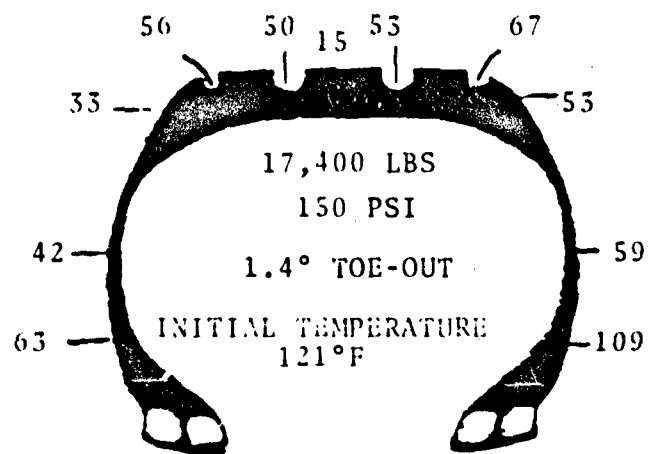
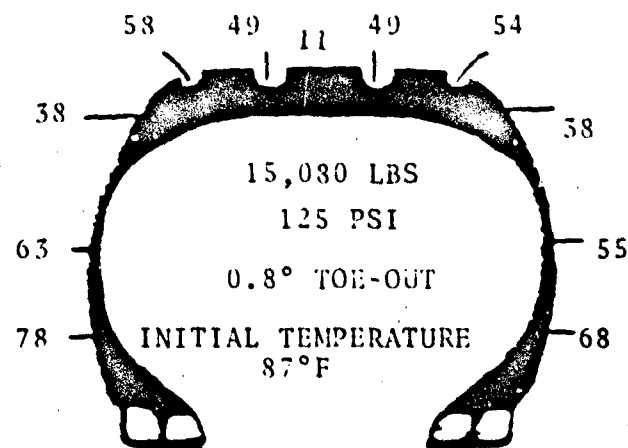


Figure 10. Taxi Test Tire Surface Temperature Rise at 0° Toe-Out



OUTBOARD

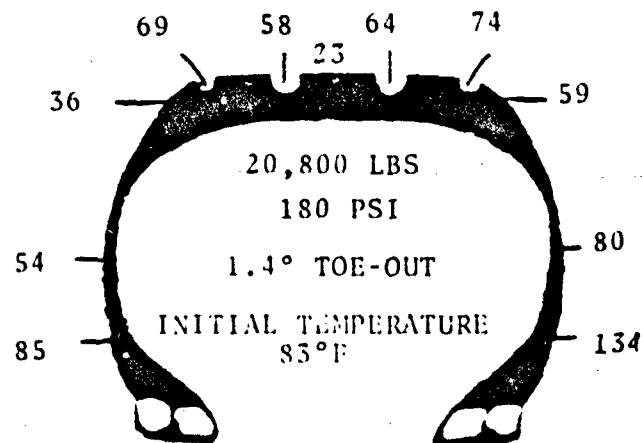
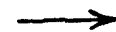


Figure 11. Taxi Test Tire Surface Temperature Rise with 0.8° and 1.4° Toe-Out

3. MYRTLE BEACH SIMULATION LABORATORY TEST

a. Approach

The objective of this testing was to duplicate in the laboratory those conditions in the field which contribute to premature A-10 tire failure. The approach was to identify the airfield that had the largest number of tire failures and to write a test plan that dynamically simulated all loads, velocities, turns, stops and distances rolled by an A-10 main landing gear tire from the time the aircraft leaves the chocks until it is airborne and from the time it lands until it returns to the chocks. These aircraft maneuvers were translated into a series of dynamics statements that were used to program the computer controlled tire test dynamometer at Wright-Patterson AFB. From the available data, it was determined that the most tire failures, on a percent basis, occurred at Myrtle Beach AFB. These tests were designed to simulate A-10 operating conditions at Myrtle Beach. Representative taxi speeds, distances, turns and stop times were determined through conversations with A-10 pilots and a scaling of the airfield map.

A summary of the test conditions is shown in Table 6. The testing sequence was: 1, 5, 2, 4, repeated 25 times for a total of 100 cycles. Then, the sequence 3, 5 was repeated 5 times for an additional 10 cycles. Tires A, B and C were tested with a fixed toe-out of 0.8 degrees, and Tire B was also tested with 0 degrees toe-out. The cornering force required for a turn was calculated by obtaining the velocity during a turn (from pilots), the radius of the turn (from the map), and using these quantities, with the aircraft gross weight in the equation for centrifugal force. The result of this calculation was used as an input to a carpet plot of cornering force versus normal load and slip angle to obtain the slip angle required to execute the turn (Appendix A). When an aircraft is operated with equal amounts of toe-out in the right and left main gear, then the straight ahead rolling condition is one of equilibrium due to cornering forces developed by the right and left tires being equal and opposite. To execute a right turn of the aircraft requires an increase in slip angle of the right wheel and an initial decrease in slip angle of the left wheel. For example, if the aircraft were operating with a toe-out of 0.8 degrees, then a right turn that requires a slip angle of 1 degree would result in an effective slip angle of 1.8 degrees on the right wheel and 0.2 degrees on the left wheel.

TABLE 6

MYRTLE-BEACH SIMULATION TEST CONDITIONS

<u>Condition</u>	Aircraft Gross Weight (Lb)	Takeoff Speed (Mph)	Touchdown Speed (Mph)	Total Distance Rolled (Ft)	Test Tire Load (Lb)	Test Tire Inflation (Psi)
1. Long Distance Taxi-Takeoff	38,000	143	--	12,400	17,000	150
2. Short Distance Taxi-Takeoff	38,000	143	--	5,700	17,000	150
3. Heavy Gross Weight Long Distance Taxi-Takeoff	48,000	188	--	14,560	22,000	180
4. Landing - Long Distance Taxi	30,000	--	150	19,450	14,000	150
5. Landing - Short Distance Taxi	30,000	--	150	12,020	14,000	150

Aircraft stop times during taxi and prior to takeoff were taken as the shortest duration usually experienced during operations. For example, if an aircraft were stopped awaiting control tower clearance for 1 to 5 minutes, then a stop duration of 1 minute was used in the test. This shorter stop time was a worst case condition as it would allow less tire cooling. Braking was not simulated because at the time this simulation was written, the dynamometer had no provisions for programmable braking. Since then, an analog computer system has been developed to interface with the digital control system of the dynamometer, and when used in conjunction with the aircraft brake can provide programmable braking.

b. Taxi Takeoff Simulation

Figure 12 shows the routes taken during the long and short distance taxi-takeoffs. If the prevailing wind is from the north, the aircraft will perform a short distance taxi-takeoff. When the wind is from the south, the aircraft will use the long distance taxi-takeoff. The major difference between the two routes is the length of taxiway travelled between the parking apron and the arming area which is approximately 6800 feet for the long distance taxi as compared to 600 feet for the short distance taxi. In either case, the aircraft will execute several low speed turns to leave the parking apron, enter the taxiway and proceed to the arming area. The aircraft then turns into the arming area and stops for two minutes to take on stores. After several low speed turns out of the arming area and back to the runway, the aircraft will make a turn at the end of the taxiway and finally another turn to the runway where it will stop for one minute prior to takeoff. The takeoff roll is the same distance for both long and short taxi-takeoff simulations as aircraft gross weight is considered equal for both conditions. For the heavy gross weight long distance taxi-takeoff, the takeoff distance and velocity are necessarily greater.

Tire surface temperatures were recorded throughout the taxi-takeoff tests. After beginning the taxi, the aircraft makes two stops: a stop for arming and a stop prior to takeoff. The tire rotation is stopped when the aircraft becomes airborne, or during the laboratory simulation when the tire is unlanded from the flywheel at takeoff speed. A comparison of Tires A, B, and C

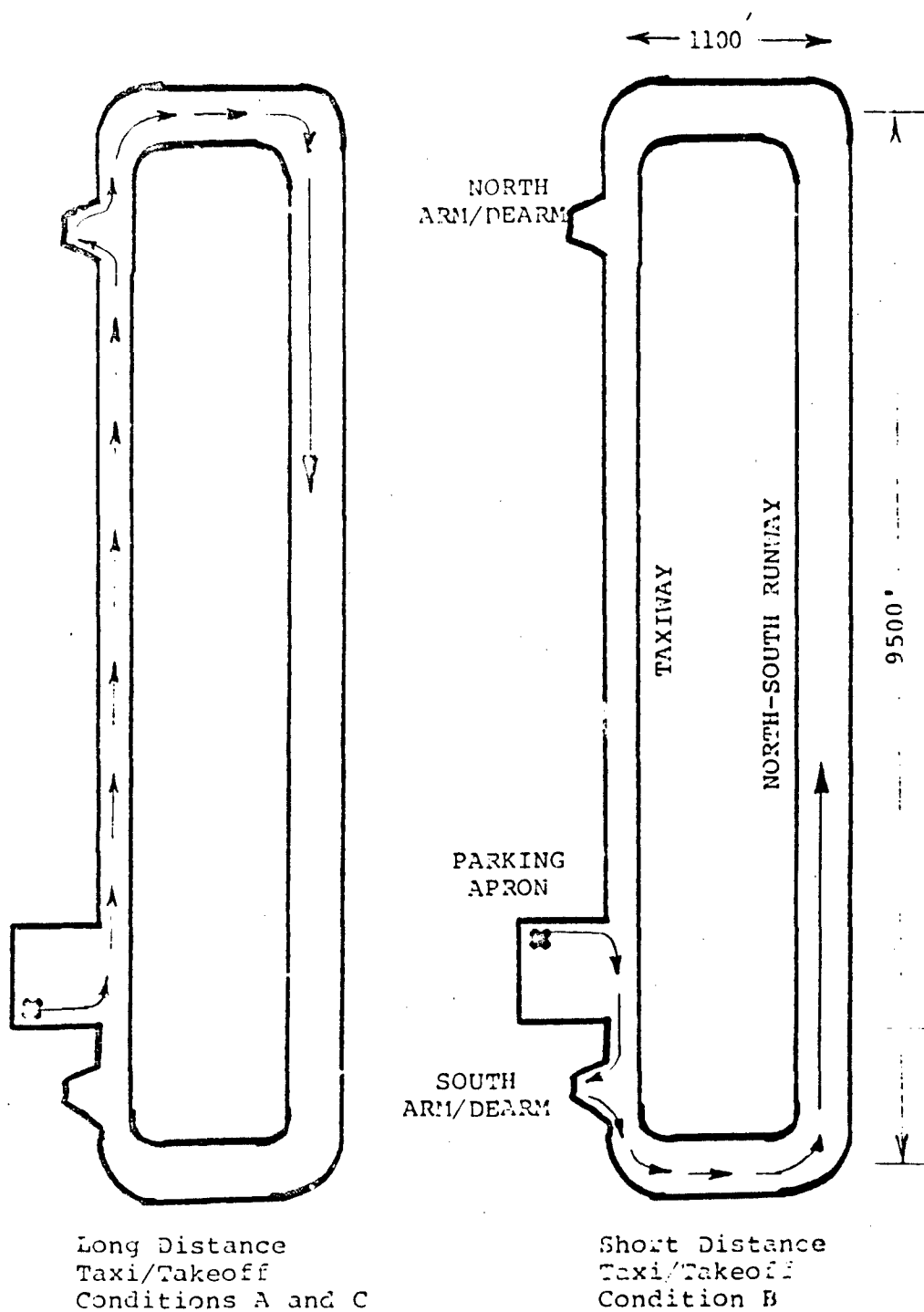


Figure 12. Taxi/Takeoff Conditions used in the Myrtle-Beach Simulation

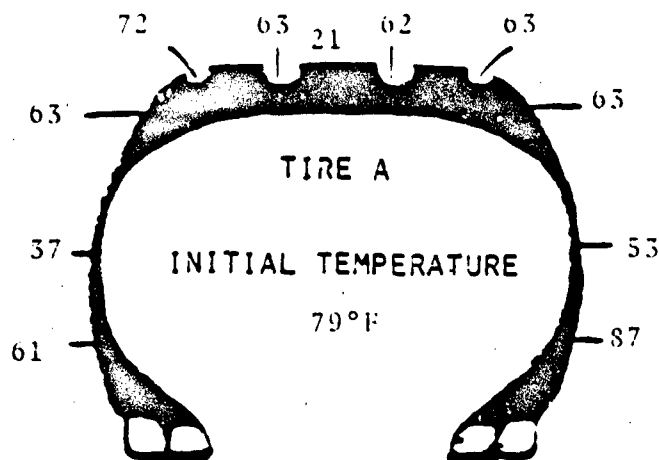
surface temperature development during the long distance taxi-takeoff simulation is shown in Figures 13 a, b, and c for the corresponding aircraft conditions of stopped for arming, stopped prior to takeoff, and airborne. Figures 14 a, b, and c are temperature profiles during the short distance taxi-takeoff simulation. Figures 15 a, b, and c are temperature profiles taken during the heavy gross weight long distance taxi-takeoff simulation. A study of Figures 13, 14, and 15 leads to the following conclusions:

- (1) All three tires experienced the smallest surface temperature rise during the short distance taxi-takeoff and the largest surface temperature rise during the heavy gross weight long distance taxi-takeoff.
- (2) The effect of operating throughout the taxi-takeoff simulations with a 0.8 degree toe-out was to cause the outboard sidewall temperature rise to be greater than the inboard sidewall temperature rise.
- (3) Tire C had a considerably lower temperature rise than tires A or B.

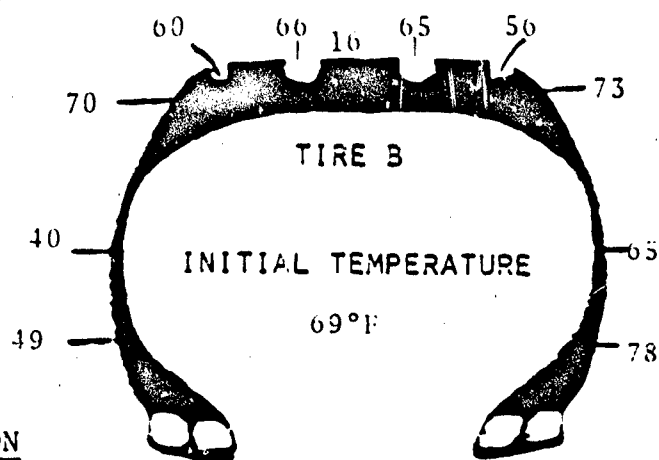
c. Landing-Taxi Simulation

Figure 16 illustrates the airfield routes taken during the landing-taxis. If the prevailing wind is from the north, the aircraft will perform a landing-long distance taxi. When the wind is from the south, the landing-short distance taxi route will be followed. For both cases, after touchdown, the pilot will decelerate the aircraft using aerodynamic speed brakes for the first 4500 feet of runway and then use minimal wheel braking for the remaining 4500 feet of runway. The aircraft will then turn off the runway onto the taxiway and make several turns entering the dearming area where it will stop for 2 minutes until the stores are removed. The aircraft will then turn out of the dearming area and taxi either 6800 or 600 feet to the parking apron, turn into the parking apron and stop.

Tire surface temperatures were recorded during the landing-taxi tests. Figures 17 a, b, and c and 18 a, b, and c were the temperature profiles for the landing-long distance taxi and landing-short distance taxi respectively. The surface temperature data shown in Figures 18 and 19 suggest the same general conclusions as reached during the taxi-takeoff tests:



TIRE CONDITIONS
17,000 LBS LOAD
150 PSI INFLATION



OUTBOARD
→

AIRCRAFT CONDITION
STOPPED FOR ARMING

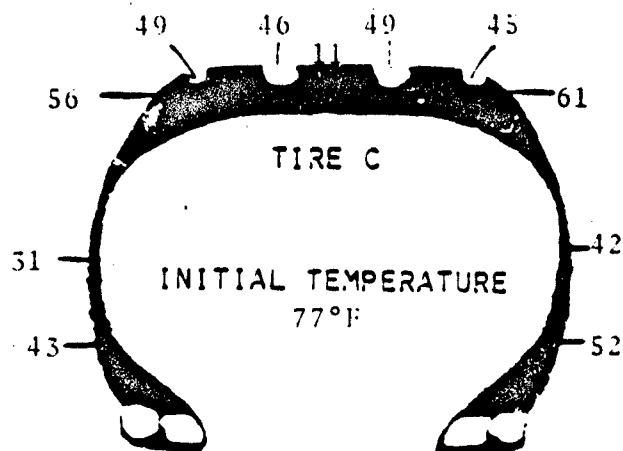
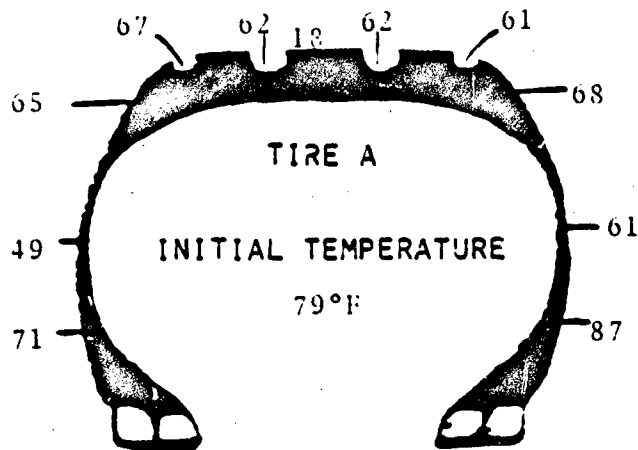
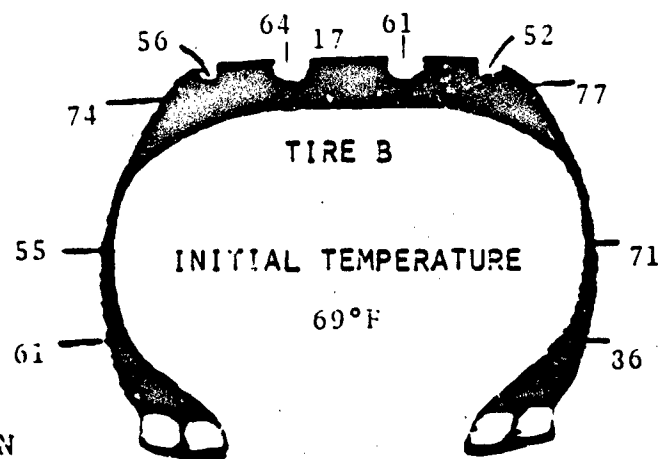


Figure 13a. Comparison of Tire Surface Temperatures During the Long Distance Taxi-Takeoff Simulation



TIRE CONDITIONS
17,000 LBS LOAD
150 PSI INFLATION



OUTBOARD



AIRCRAFT CONDITION
STOP BEFORE TAKEOFF

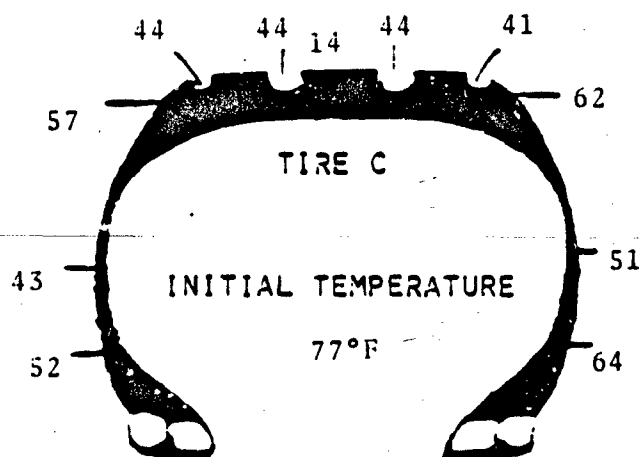
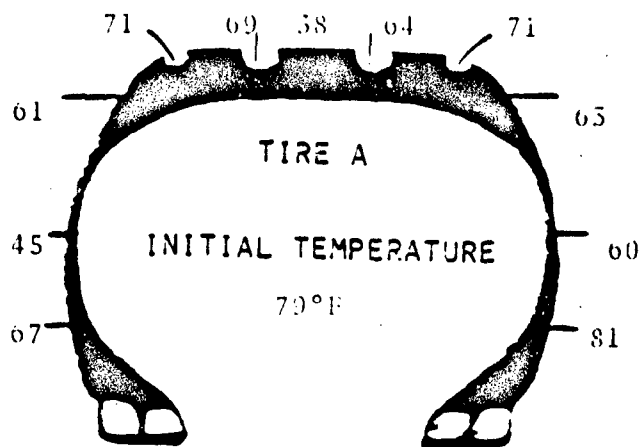
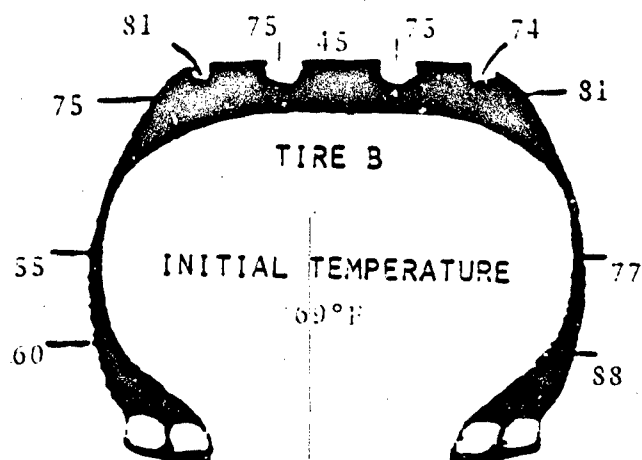


Figure 13b. Stop Before Takeoff

TIRE CONDITIONS
17,000 LBS LOAD
150 PSI INFLATION



AIRCRAFT CONDITION
AIRBORNE



OUTBOARD

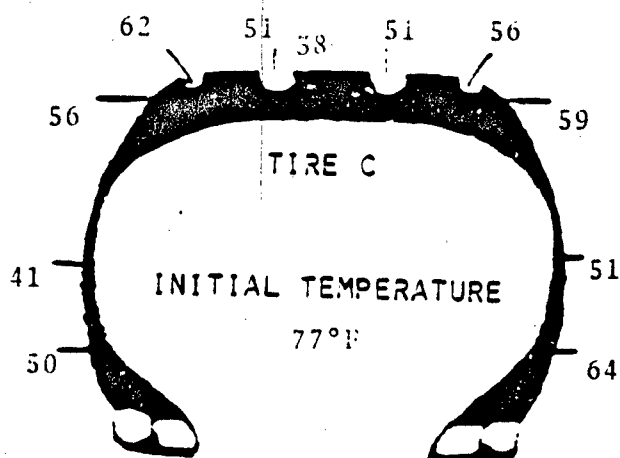
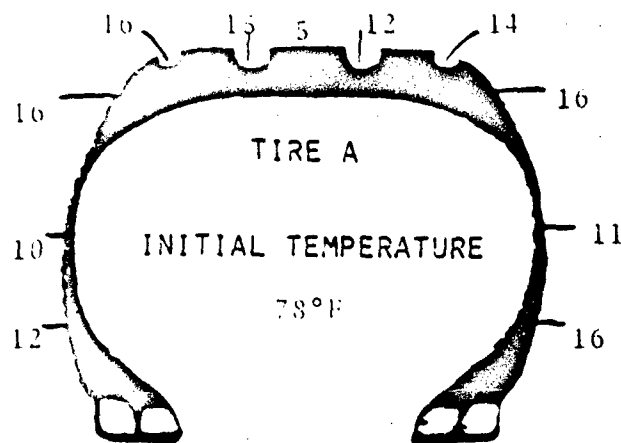
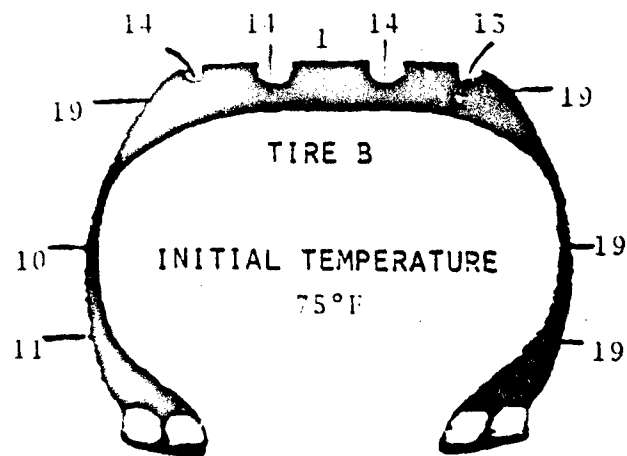


Figure 13c. Airborne



TIRE CONDITIONS
17,000 LBS LOAD
150 PSI INFLATION



OUTBOARD



AIRCRAFT CONDITION
STOPPED FOR ARMING

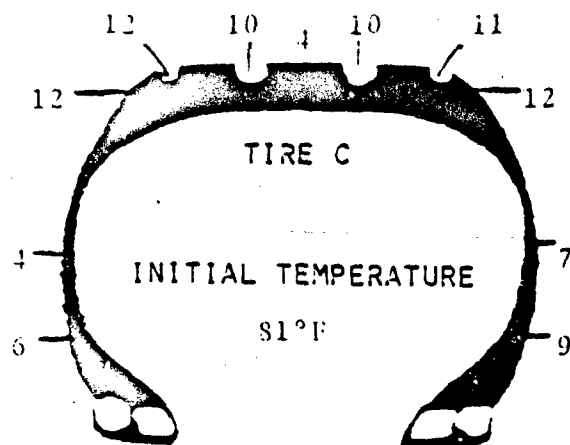
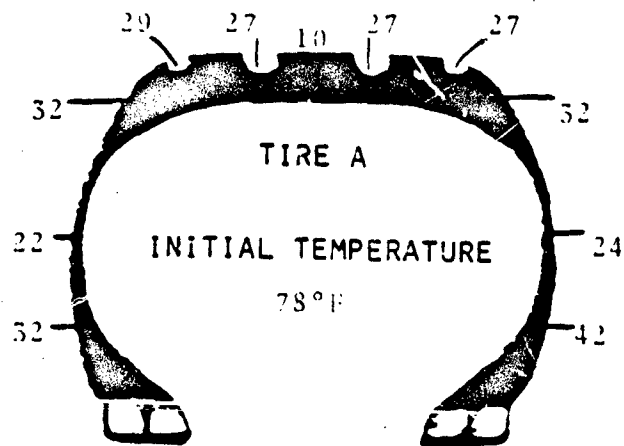
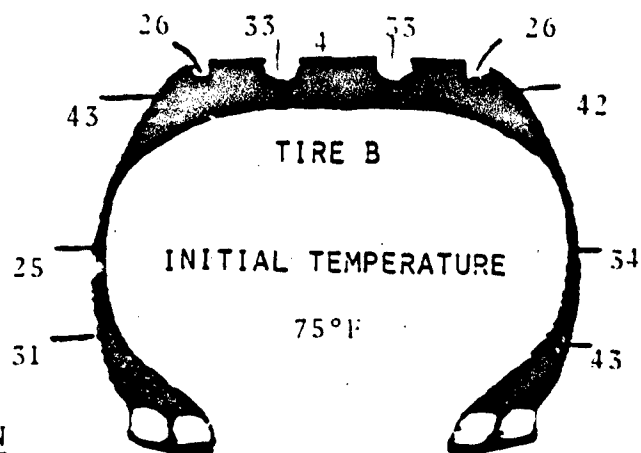


Figure 14a. Comparison of Tire Surface Temperature Rise During the Short Distance Taxi-Takeoff Simulation



TIRE CONDITIONS
17,000 LBS LOAD
150 PSI INFLATION



OUTBOARD



AIRCRAFT CONDITION
STOP BEFORE TAKEOFF

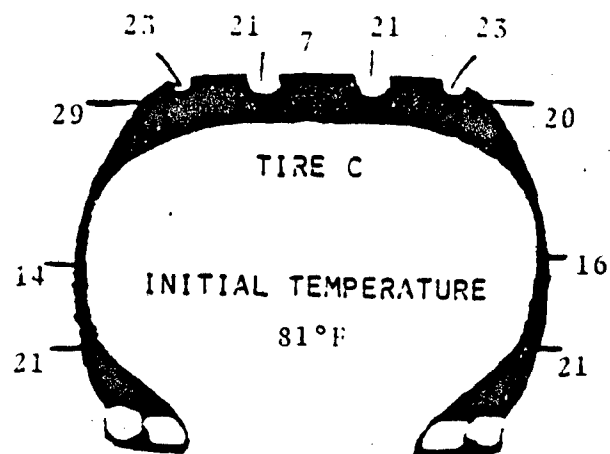
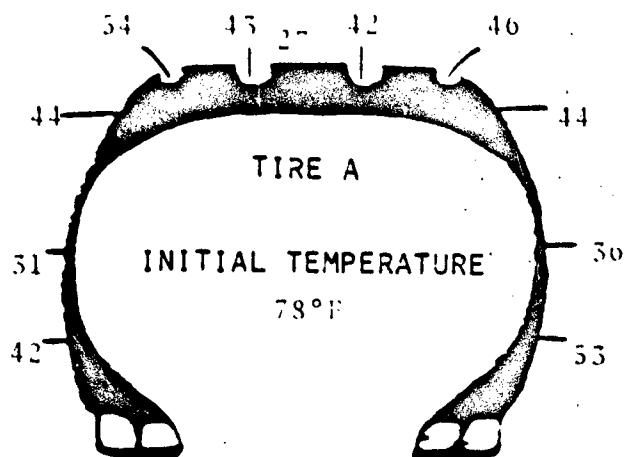
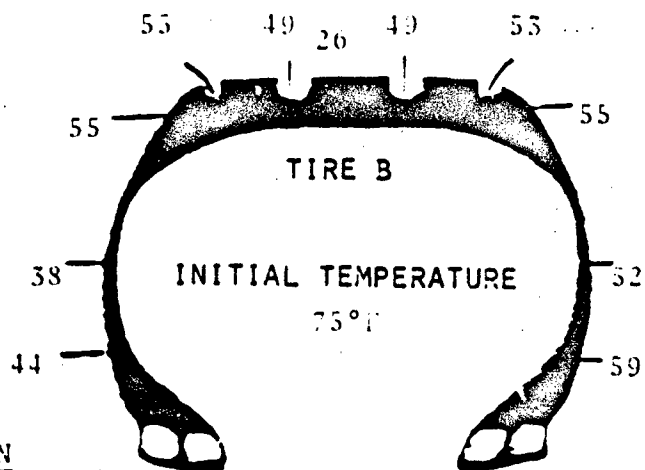


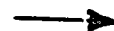
Figure 14b. Stop Before Takeoff



TIRE CONDITIONS
 17,000 LBS LOAD
 150 PSI INFLATION



OUTBOARD



AIRCRAFT CONDITION
 AIRBORNE

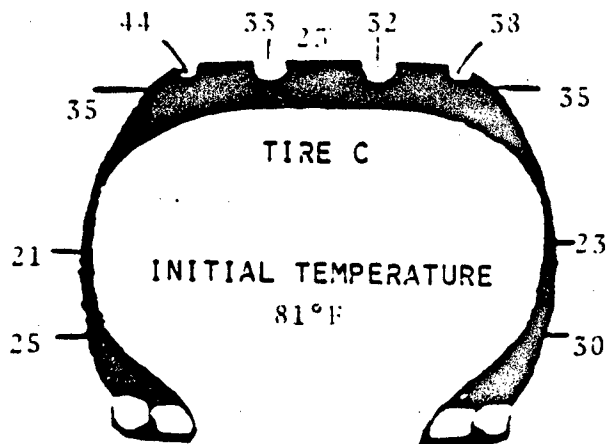
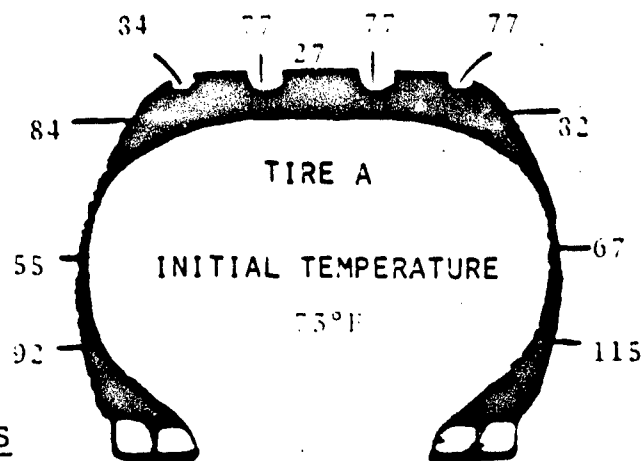
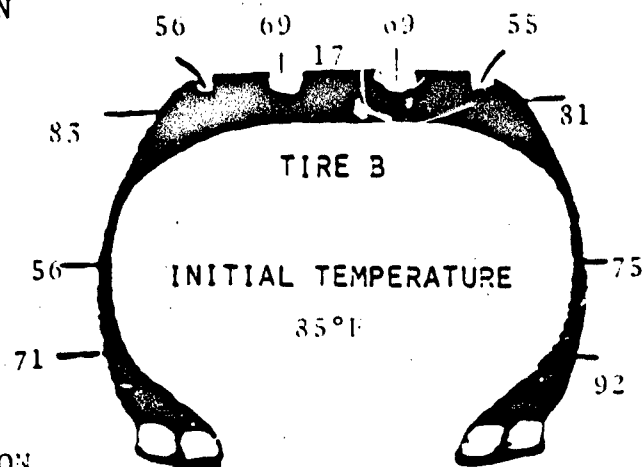


Figure 14c. Airborne



TIRE CONDITIONS
22,000 LBS LOAD
180 PSI INFLATION



OUTBOARD
→

AIRCRAFT CONDITION
STOPPED FOR ARMING

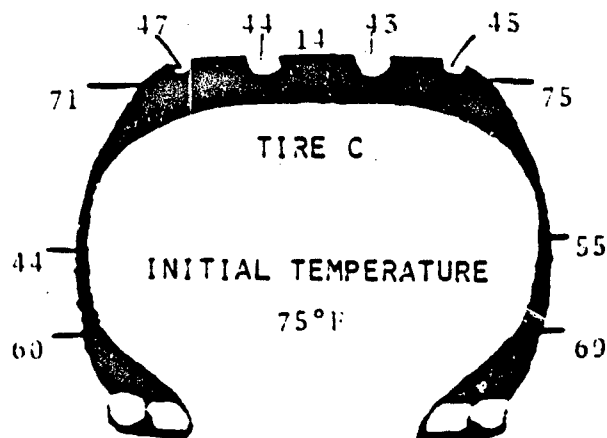
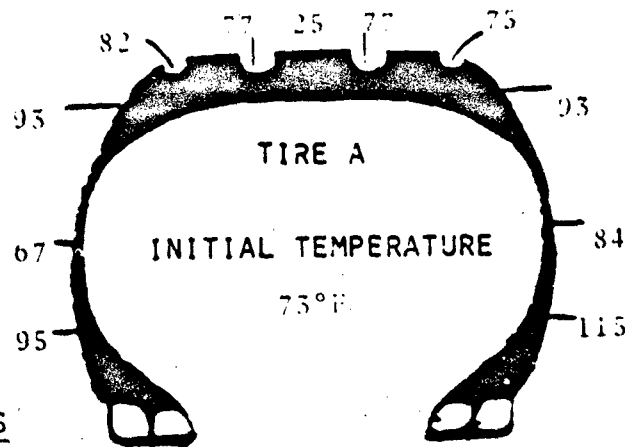
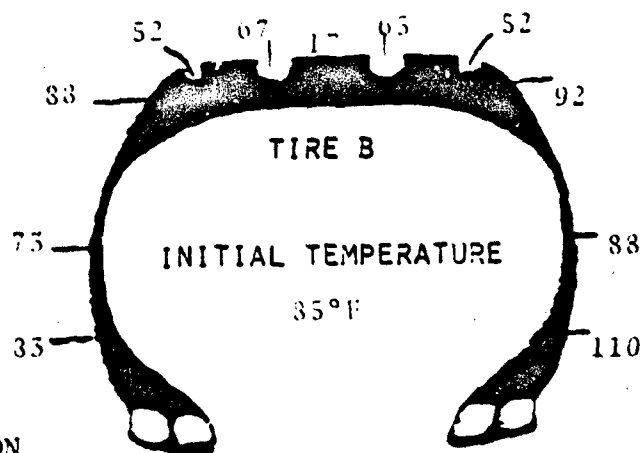


Figure 15a. Comparison of Tire Surface Temperature Rise During the Heavy Gross Weight Long Distance Taxi-Takeoff Simulation



TIRE CONDITIONS
22,000 LBS LOAD
180 PSI INFLATION



OUTBOARD
→

AIRCRAFT CONDITION
STOP BEFORE TAKEOFF

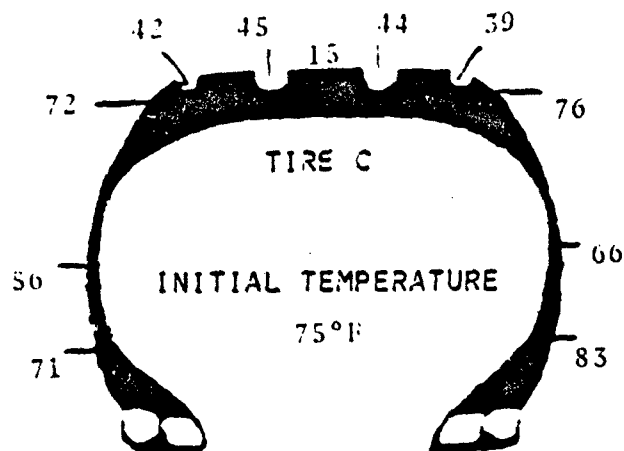
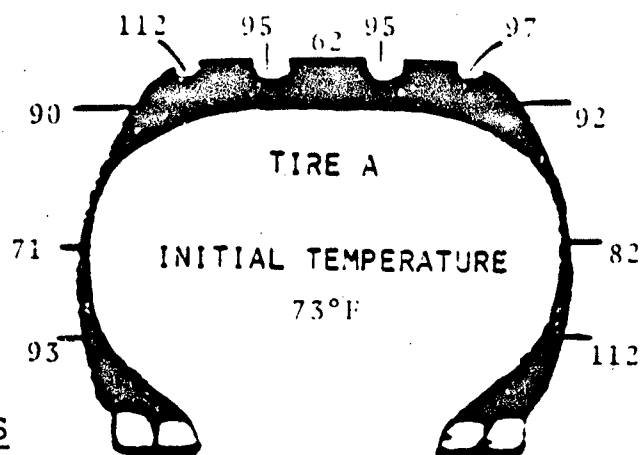
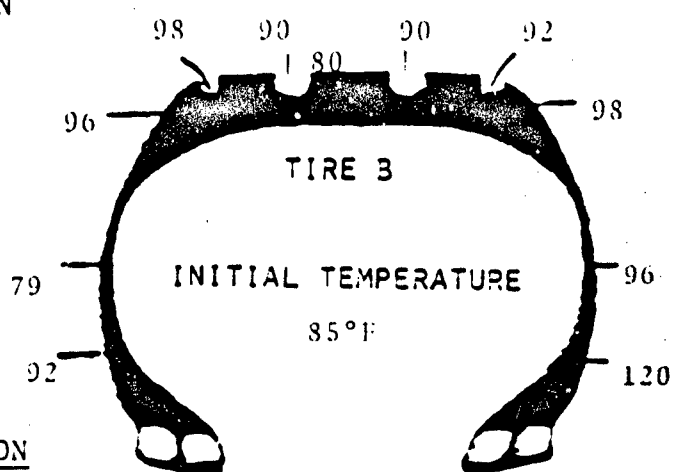


Figure 15b. Stop Before Takeoff

TIRE CONDITIONS
 22,000 LBS LOAD
 180 PSI INFLATION



AIRCRAFT CONDITION
 AIRBORNE



OUTBOARD

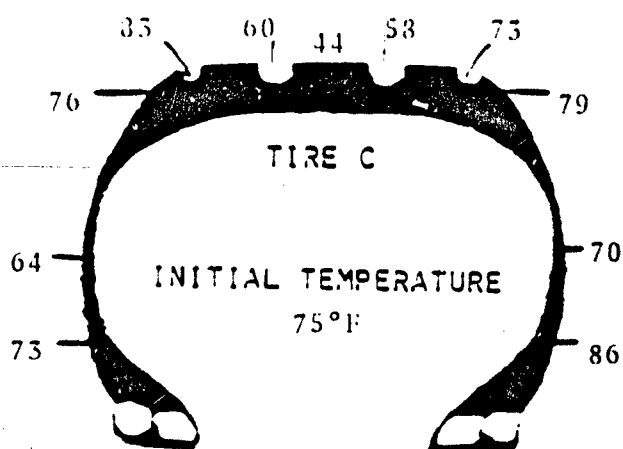
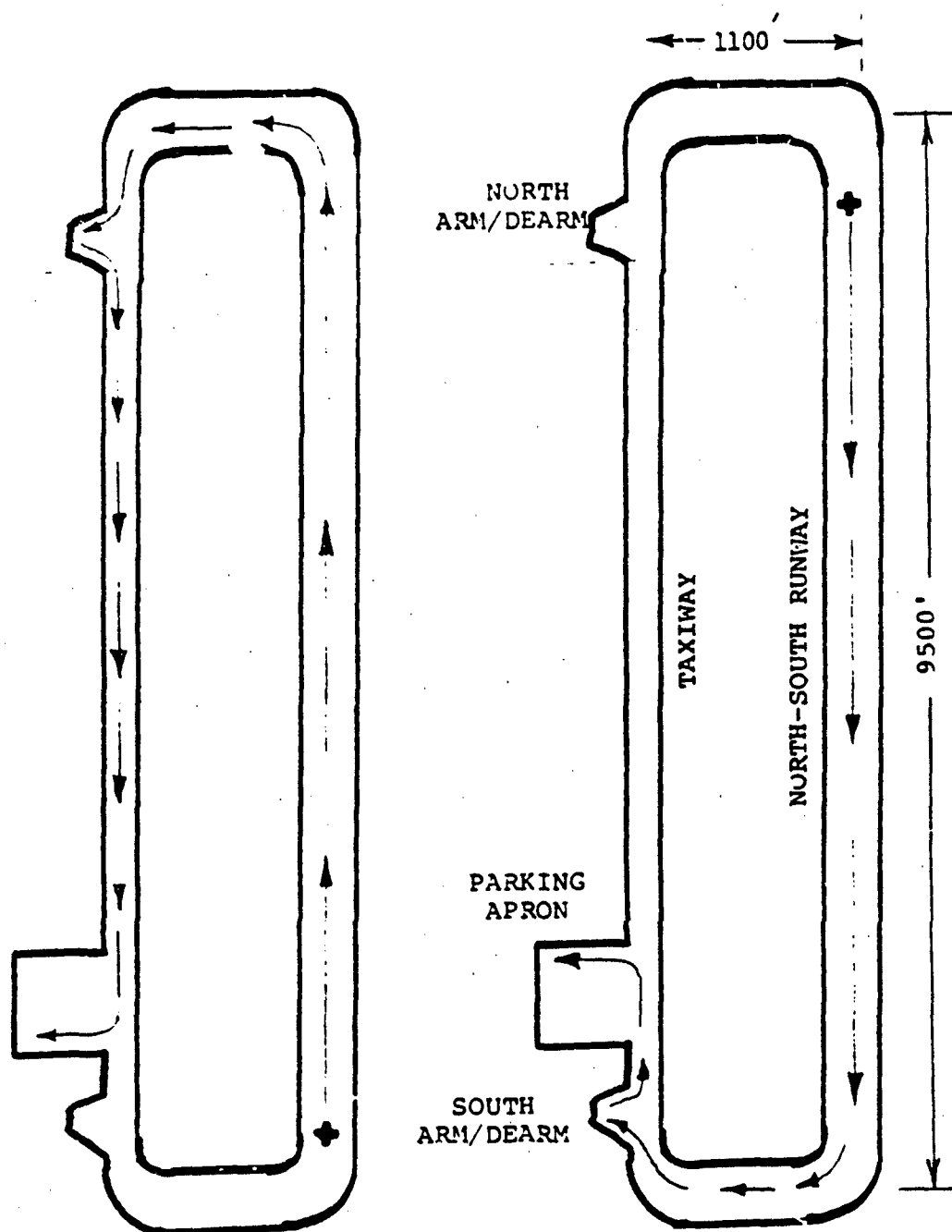


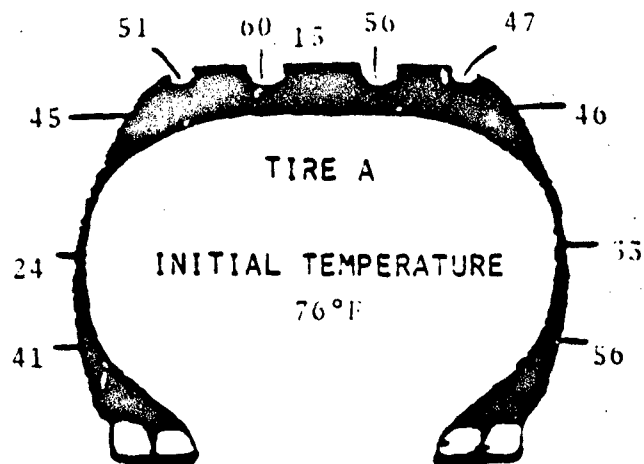
Figure 15c. Airborne



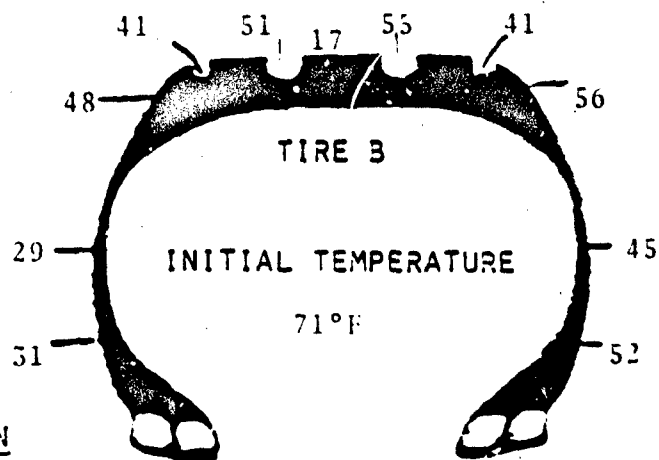
Landing/Long Distance Taxi
Condition D

Landing/Short Distance Taxi
Condition E

Figure 16. Landing/Taxi Conditions used in the Myrtle-Beach Simulation



TIRE CONDITIONS
 15,400 LBS LOAD
 150 PSI INFLATION



OUTBOARD



AIRCRAFT CONDITION
 AFTER LANDING ROLL

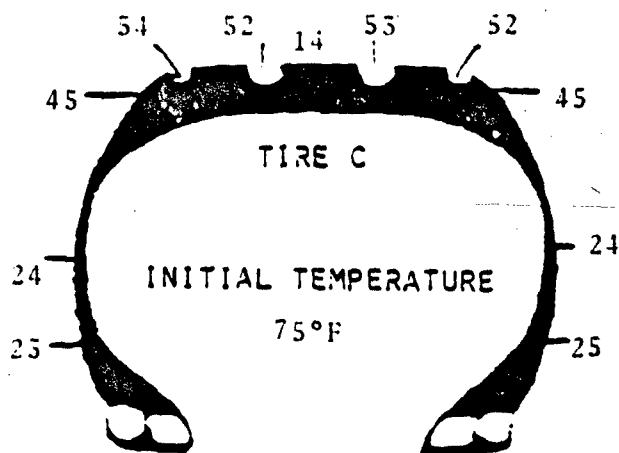
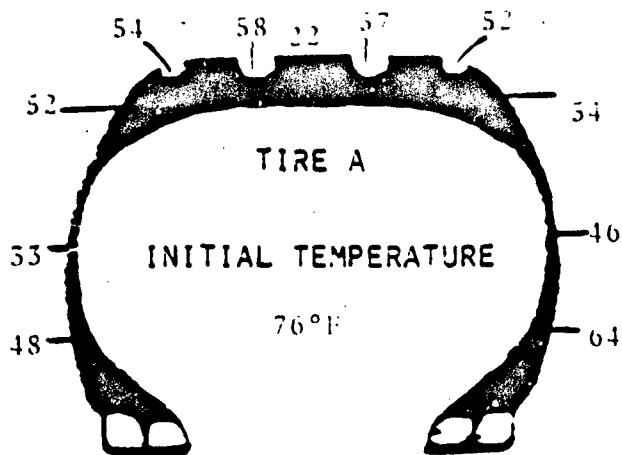
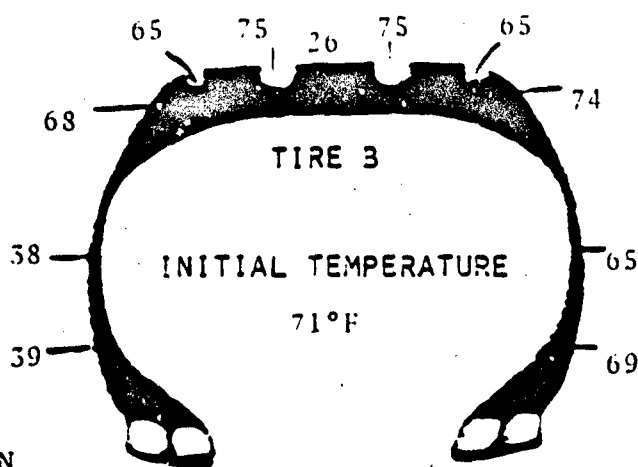


Figure 17a. Comparison of Tire Surface Temperatures During the Landing-Short Distance Taxi Simulation



TIRE CONDITIONS
 15,400 LBS LOAD
 150 PSI INFLATION



OUTBOARD
 →

AIRCRAFT CONDITION
 STOP FOR DEARMING

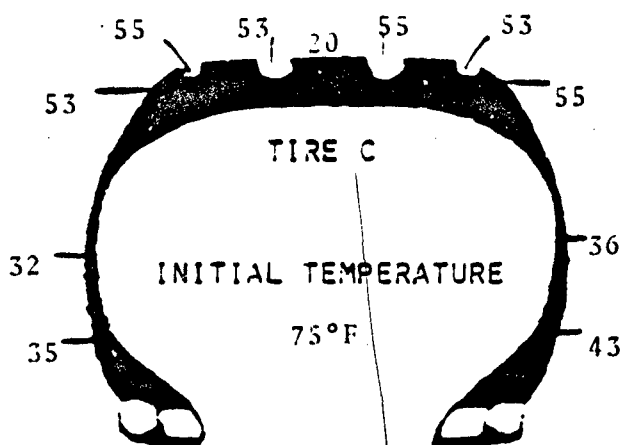
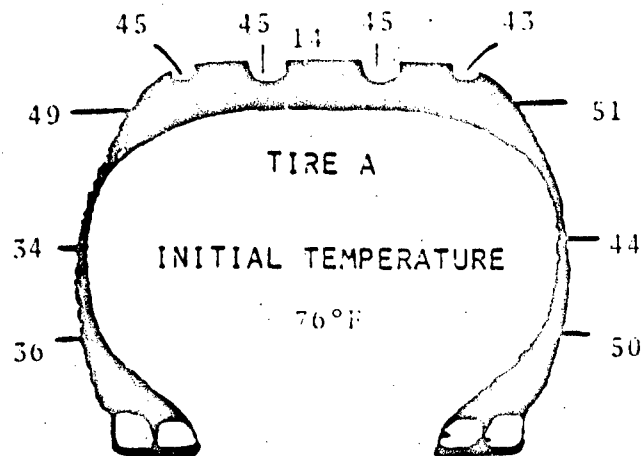
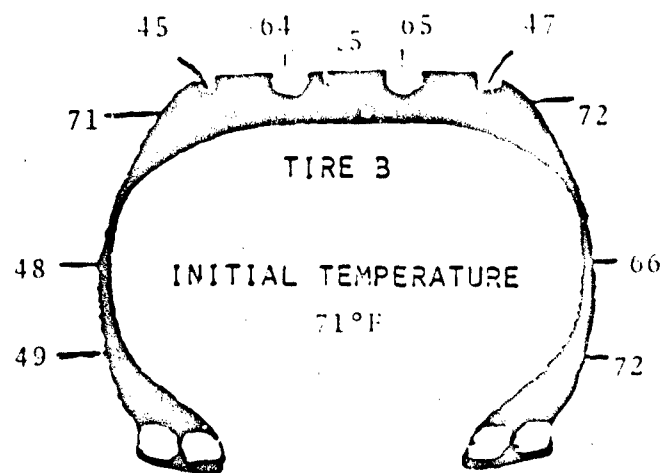


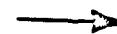
Figure 17b. Stop for Darming



TIRE CONDITIONS
 15,400 LBS LOAD
 150 PSI INFLATION



OUTBOARD



AIRCRAFT CONDITION
 PARKED

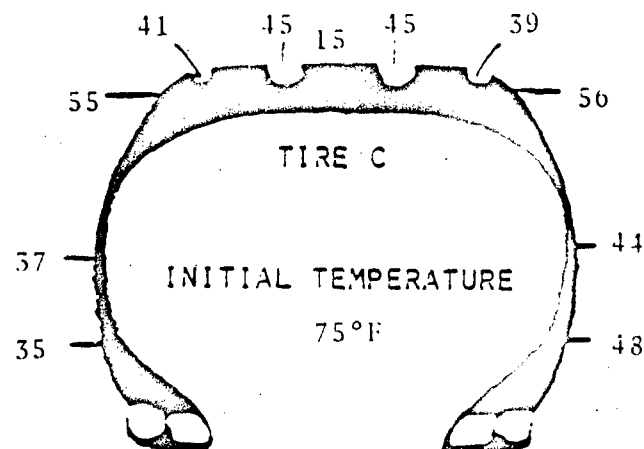
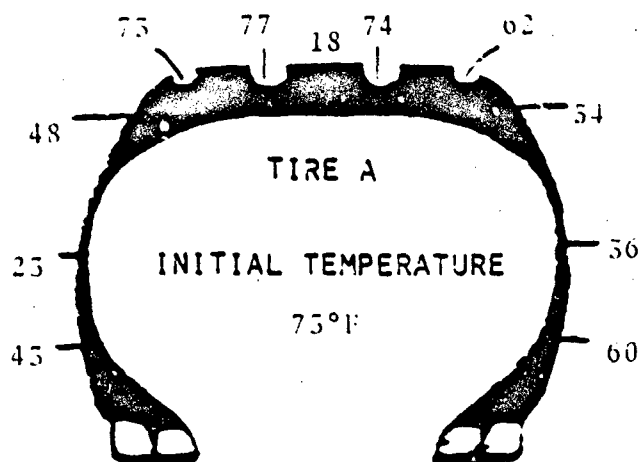


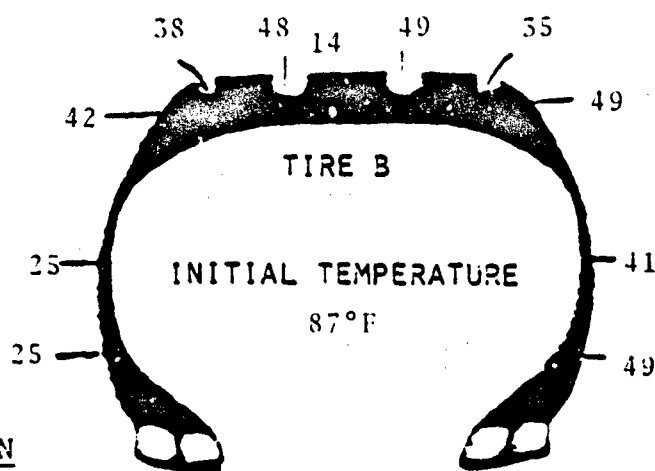
Figure 17c. Parked



TIRE CONDITIONS

.5,400 LBS LOAD

.50 PSI INFLATION



OUTBOARD



AIRCRAFT CONDITION

AFTER LANDING ROLL

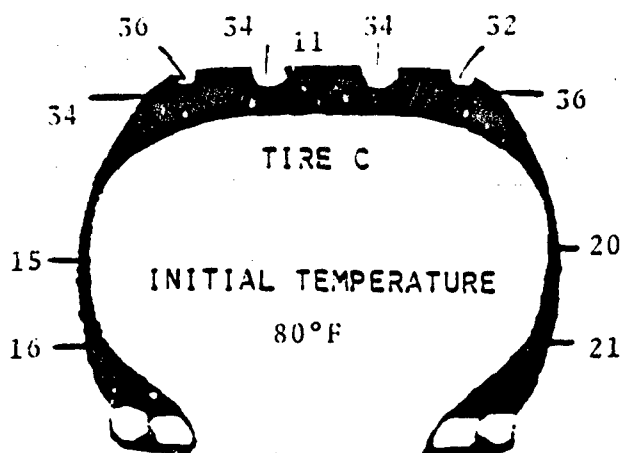
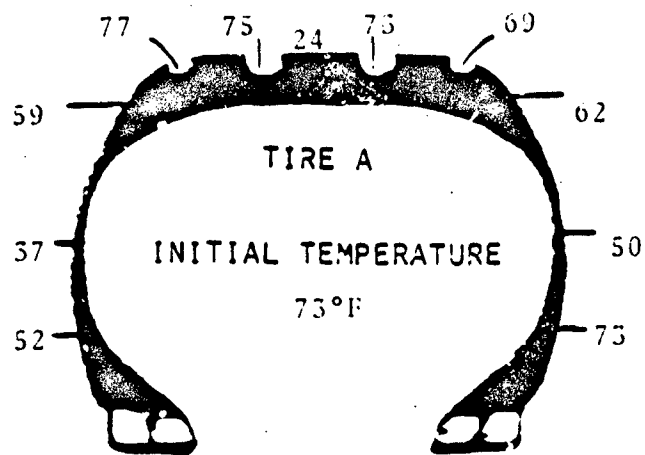
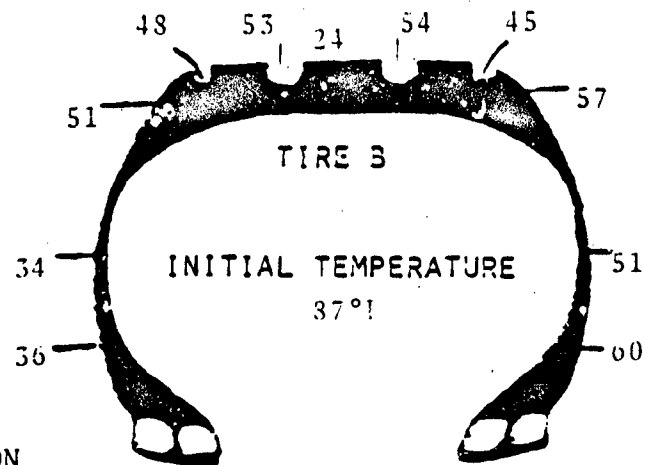


Figure 18a. Comparison of Tire Surface Temperature Rise During the Landing-Long distance Taxi Simulation



TIRE CONDITIONS
 15,400 LBS LOAD
 150 PSI INFLATION



AIRCRAFT CONDITION
 STOP FOR DEARMING

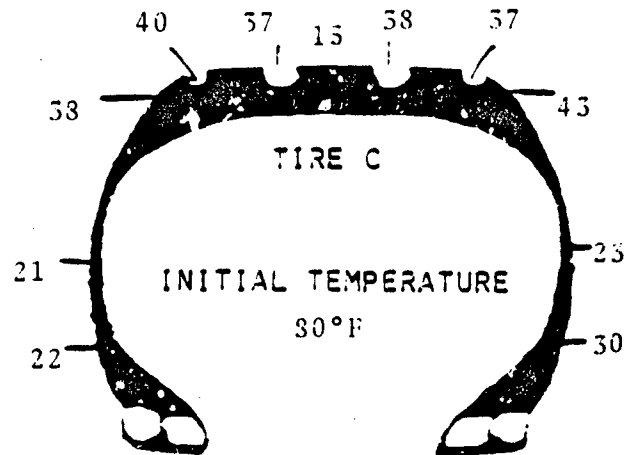
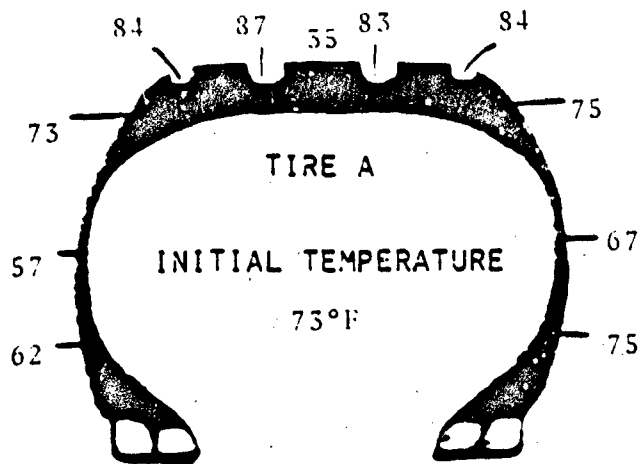


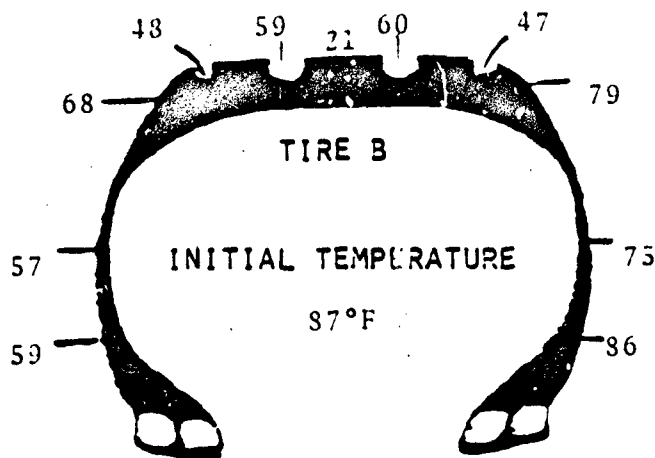
Figure 18b. Stop for Dearming



TIRE CONDITIONS

15,400 LBS LOAD

150 PSI INFLATION



OUTBOARD



AIRCRAFT CONDITION

PARKED

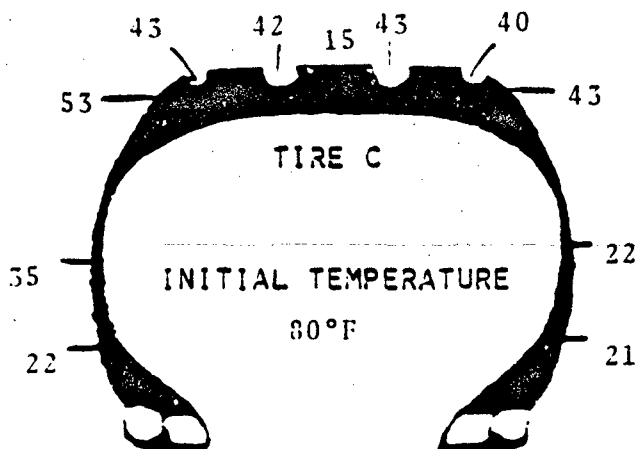


Figure 18c. Parked

(1) A smaller surface temperature rise was developed by all three tires during the landing-short distance taxi test.

(2) The 0.8 degree toe-out caused the outboard sidewall to run hotter than the inboard sidewall.

(3) Tire C ran considerably cooler than either Tires A or B.

d. Simulation with 0 Degrees Toe-Out

All the preceding laboratory simulation tests were conducted with 0.8 degrees toe-out. To better assess the effect of the toe-out, these tests were repeated on Tire B with 0 degree toe-out. As discussed earlier, this will not only change the tire straight ahead rolling conditions, but also, slip angles during the turns: 0.8 degree was subtracted from the previously calculated slip angles for right turns and added to those values that were calculated for left turns. All other distances, velocities and stop times remained the same as they were during the simulation with 0.8 degree toe-out. Figures 19 - 23 inclusive show the surface temperature profiles at the end of the test run (airborne for taxi-takeoff tests and parked for landing-taxi tests). Temperature profiles of Tire B with 0.8 degree toe-out were included on the same Figure for ease of comparison. As seen in Figures 19 - 23, the effect of toe-out on tire surface temperature rise was:

(1) When operating with 0 degree toe-out, the outboard and inboard sidewall temperature rise was approximately equal.

(2) The tread surface temperature distribution was unaffected by a small toe-out angle.

e. Tire Failures During the Simulation Tests

Since the primary goal of the simulation tests was to duplicate in the laboratory those conditions in the field which contribute to tire failure, the tests were repeated until a tire failed or had attained 220 cycles of testing. The testing sequence follows (refer to Table 6):

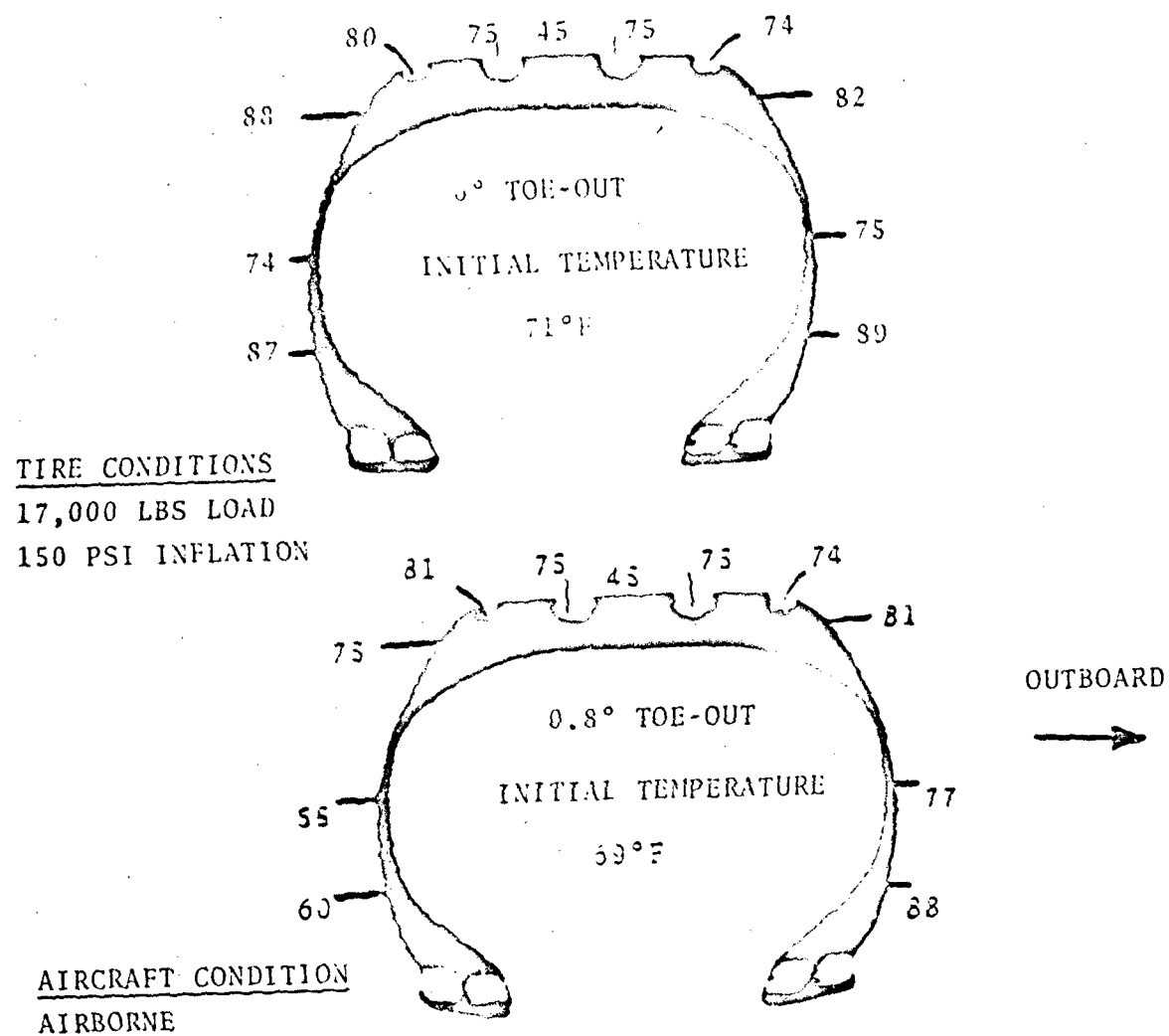
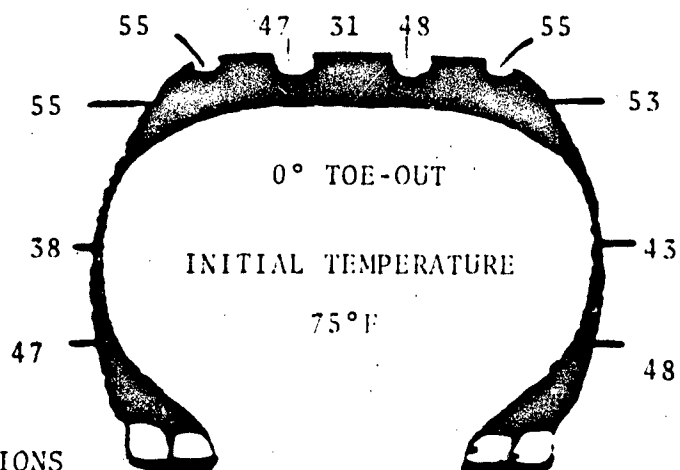


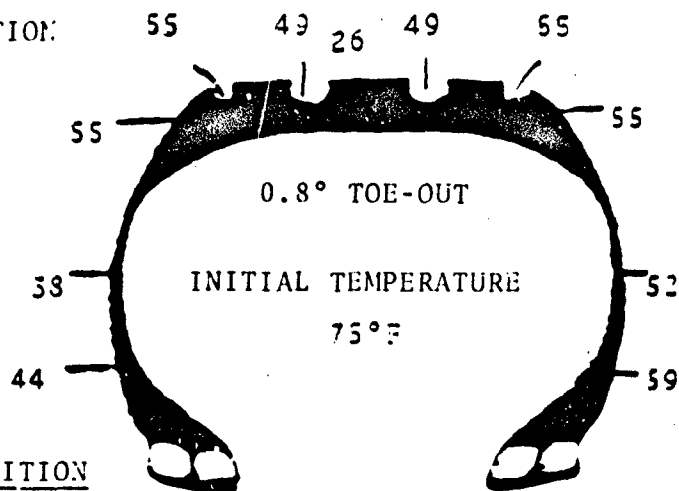
Figure 19. Comparison of Tire B Surface Temperatures with 0.8° and 0° Toe-Out During the Long Distance Taxi-Takeoff Simulation



TIRE CONDITIONS

17,000 LBS LOAD

150 PSI INFLATION



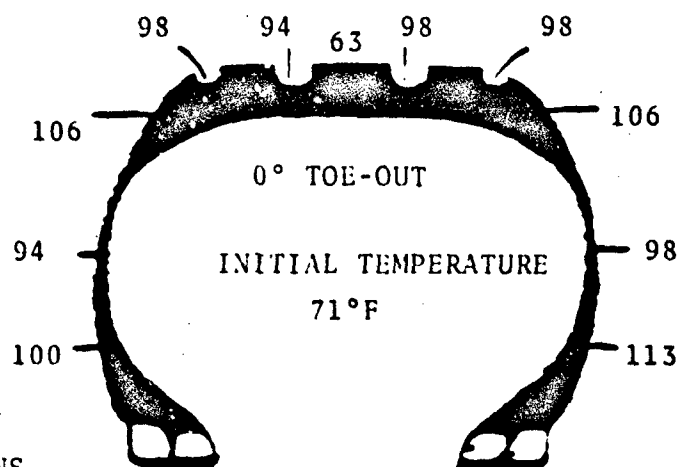
OUTBOARD



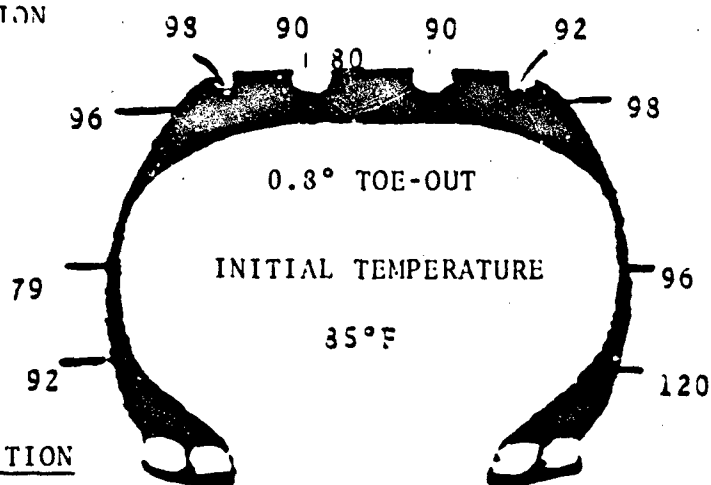
AIRCRAFT CONDITION

AIRBORNE

Figure 20. Comparison of Tire B Surface Temperatures with 0.8° and 0° Toe-Out During the Short Distance Taxi-Takeoff Simulation



TIRE CONDITIONS
22,000 LBS LOAD
180 PSI INFLATION

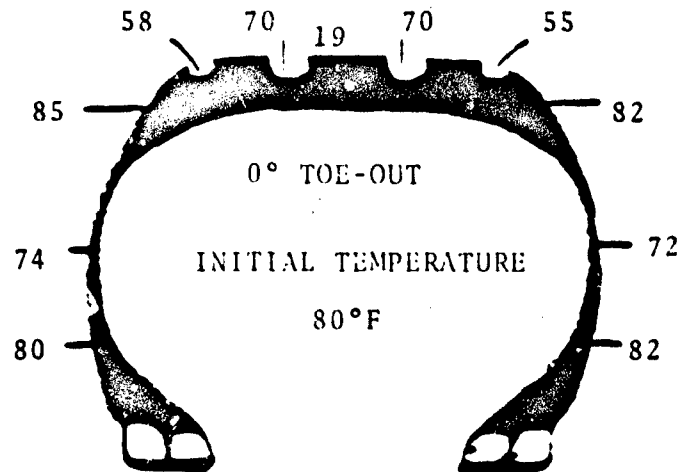


OUTBOARD

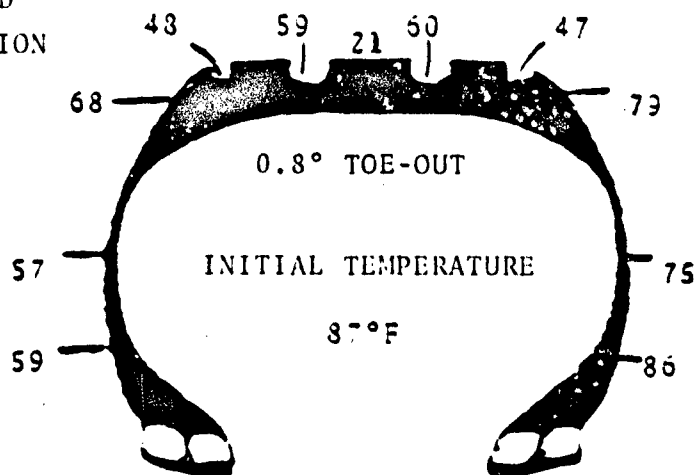


AIRCRAFT CONDITION
AIRBORNE

Figure 21. Comparison of Tire B Surface Temperatures with 0.8° and 0° Toe-Out During the Heavy Gross Weight Long Distance Taxi-Takeoff Simulation



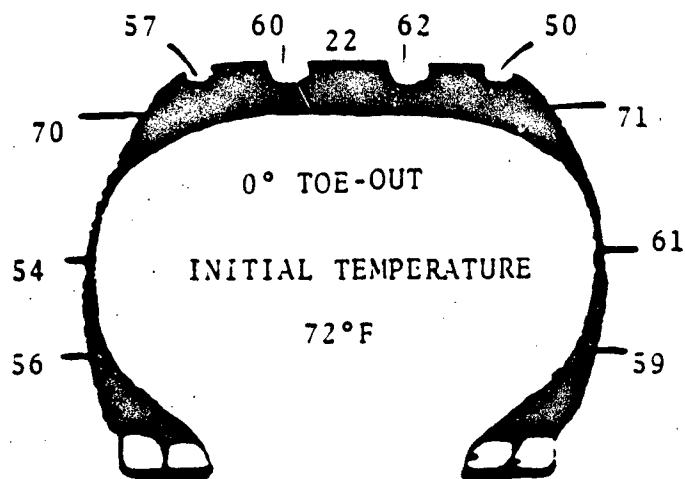
TIRE CONDITIONS
 15,400 LBS LOAD
 150 PSI INFLATION



OUTBOARD
 →

AIRCRAFT CONDITION
 PARKED

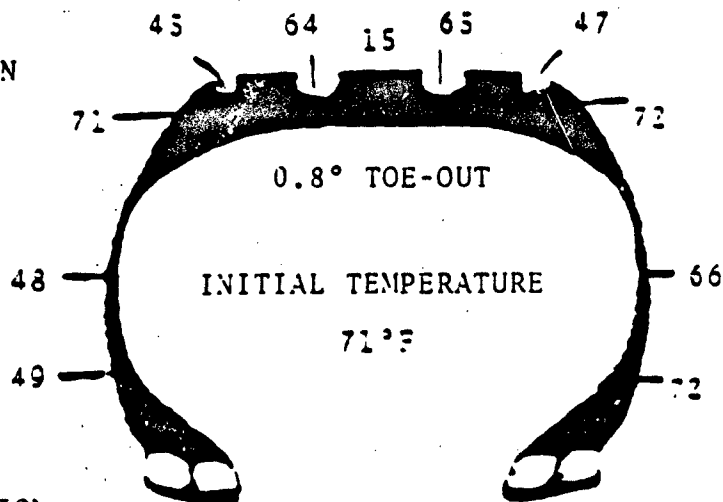
Figure 22. Comparison of Tire B Surface Temperatures with 0.8° and 0° Toe-Out During the Landing-Long Distance Taxi Simulation



TIRE CONDITIONS

15,400 LBS LOAD

150 PSI INFLATION



OUTBOARD



AIRCRAFT CONDITION

PARKED

Figure 23. Comparison of Tire B Surface Temperatures with 0.8° and 0° Toe-Out During the Landing-Short Distance Taxi Simulation

Long Distance Taxi-Takeoff
 Landing-Short Distance Taxi
 Short Distance Taxi-Takeoff
 Landing-Long Distance Taxi

which was repeated 25 times for a total of 100 cycles. Then the sequence:

Heavy Gross Weight Long Distance Taxi-Takeoff
 Landing-Short Distance Taxi

was repeated 5 times for an additional 10 cycles. After a tire had completed the first 110 cycles, then the procedure was repeated. The 220 cycles of laboratory testing correspond to 110 landings in the field and were a reasonable expectation for tires operating under these conditions. The tire performance data are summarized in Table 7.

TABLE 7

TIRE PERFORMANCE DURING THE
 MYRTLE BEACH SIMULATION TESTS

<u>TIRE</u> <u>TYPE</u>	<u>TEST CYCLES</u> <u>COMPLETED</u>	<u>FAILURE MODE</u>
A	100	Blowout at Shoulder
B	220	---
C	220	---
A - Retread	103	Air Leak at Vent Holes
A	220	---
B	220	---

The tires were tested in the order shown in Table 7. The first Tire A developed a bulge near the shoulder that was observed by the tire test technicians at the 98th test cycle and failed during the first heavy gross weight cycle (101st cycle) by a blowout which developed at the bulge. Tire B completed 220 cycles

without any evidence of incipient failure as did Tire C. After the 103rd cycle, a recapped Tire A failed by its inability to contain air through excessive leakage at the vent holes. A different Tire A was then tested and completed the 220 cycles. A different Tire B was also tested and completed the 220 cycles.

Although only a limited number of tires could be tested, the laboratory failure data in Table 7 appears to reflect the field failure data in Table 1.

SECTION V

CORRELATION OF RESULTS

1. AVERAGE TIRE SURFACE TEMPERATURES

The surface temperature measurements presented earlier in this report were for eleven points on the tire. To better correlate the diverse range of test conditions, the following average temperatures were considered:

(1) Average Tread Temperature Rise - This temperature was the average of the four tread grooves. The center rib temperatures were not considered because they were uniformly low for all tires during the testing.

(2) Average Outboard Sidewall Temperature Rise - This temperature was the average of the outboard shoulder, apex region and minimum sidewall temperature.

(3) Average Inboard Sidewall Temperature Rise - Same as (2) but with corresponding measurements of the inboard sidewall.

(4) Average Tire Temperature Rise - This was the average of the four tread and six sidewall temperatures.

These average temperatures were listed for all test conditions in Table 8.

To partially account for the different test conditions, the temperatures reached during the tests were compared with the primary quantities of load times distance. Figure 24, 25, and 26 were plots of the average tire surface temperature rise as a function of load in thousands of pounds multiplied by distance in miles (KLB-MI) for the roll to failure and five simulation tests of Tires A, B and C. Figure 24, the Tire A plot, shows that most of the simulation points lie on or near the roll to failure curve. The heavy gross weight long distance taxi-takeoff simulation data points were considerably higher than the corresponding points on the roll to failure curve. The Tire B plot showed that most of the data from the simulation had higher temperature rises than that exhibited during the roll to failure test (Figure 25). The Tire C plot had only one point from the simulation test that was appreciably higher than the roll to failure curve

TABLE 8

AVERAGE TIRE SURFACE TEMPERATURE
RISE (°F) DURING LABORATORY AND
FIELD TESTING

<u>EST CONDITION</u>	<u>TIRE ID</u>	<u>REFERENCE FIGURE</u>	<u>TREAD</u>	<u>OUTBOARD SIDEWALL</u>	<u>INBOARD SIDEWALL</u>	<u>TIRE AVERAGE</u>
OLL TO FAILURE: After 1 Mile)	A	3	42	45	40	43
	B	4	34	41	36	37
	C	5	38	43	46	42
After 3 Miles)	A	3	79	77	71	76
	B	4	72	74	67	71
	C	5	64	72	63	66
Prior to Failure)	A	3	90	93	81	88
	B	4	84	95	81	87
	C	5	78	93	81	77
TAXI TEST:						
1°, 15,080 LBS, 125 PSI	A	10	51	78	51	59
1°, 17,400 LBS, 150 PSI	A	10	52	73	51	58
1°, 20,800 LBS, 180 PSI	A	10	62	84	53	62
1.8°, 15,080 LBS, 125 PSI	A	11	53	54	60	55
1.4°, 17,400 LBS, 150 PSI	A	11	57	74	46	58
1.4°, 20,800 LBS, 180 PSI	A	11	66	91	58	71

TABLE 8 (Continued)

	<u>TIRE</u> <u>ID</u>	<u>REFERENCE</u> <u>FIGURE</u>	<u>TREAD</u>	<u>OUTBOARD</u> <u>SIDEWALL</u>	<u>INBOARD</u> <u>SIDEWALL</u>	<u>TIRE</u> <u>AVERAGE</u>
LONG DISTANCE						
TAXI - TAKEOFF:	A	13a	65	68	54	62
(Stopped for Arming)	B	13a	62	72	53	62
	C	13a	47	52	43	47
(Stop Before Takeoff)	A	13b	63	72	62	65
	B	13b	58	78	63	65
	C	13b	43	59	51	50
(Airborne)	A	13c	69	68	58	65
	B	13c	76	82	63	74
	C	13c	55	58	49	54
SHORT DISTANCE						
TAXI - TAKEOFF:	A	14a	14	14	13	14
(Stopped for Arming)	B	14a	14	19	13	15
	C	14a	11	9	7	9
(Stop Before Takeoff)	A	14b	28	33	29	29
	B	14b	30	40	33	34
	C	14b	22	19	21	21
(Airborne)	A	14c	46	44	39	44
	B	14c	52	55	46	51
	C	14c	37	29	27	35

TABLE 8 (Continued)

<u>TEST CONDITION</u>	<u>TIRE ID</u>	<u>REFERENCE FIGURE</u>	<u>TREAD</u>	<u>OUTBOARD SIDEWALL</u>	<u>INBOARD SIDEWALL</u>	<u>TIRE AVERAGE</u>
EAVY GROSS WEIGHT ONG DISTANCE AXI - TAKEOFF:						
	A	15a	79	88	77	81
Stopped for Arming)	B	15a	62	83	70	71
	C	15a	45	66	58	55
	A	15b	78	97	85	86
(Stop Before Takeoff)	B	15b	59	97	81	77
	C	15b	43	75	66	59
	A	15c	100	95	85	94
(Airborne)	B	15c	93	105	89	95
	C	15c	69	78	71	72
LANDING - LONG DISTANCE TAXI:						
	A	17a	72	50	38	55
(After Landing Roll)	B	17a	43	46	31	40
	C	17a	34	26	22	28
	A	17b	74	62	49	63
(Stop for Dearming)	B	17b	50	56	40	49
	C	17b	38	32	27	33
	A	17c	85	72	64	75
(Parked)	B	17c	54	80	61	64
	C	17c	42	37	29	36

TABLE 8 (Concluded)

<u>TEST CONDITION</u>	<u>TIRE ID</u>	<u>REFERENCE FIGURE</u>	<u>TREAD</u>	<u>OUTBOARD SIDEWALL</u>	<u>INBOARD SIDEWALL</u>	<u>TIRE AVERAGE</u>
LANDING - SHORT						
DISTANCE TAXI:	A	18a	54	45	37	46
(After Landing Roll)	B	18a	47	51	36	45
	C	18a	53	31	31	40
(Stop for Dearing)	A	18b	55	55	44	52
	B	18b	70	69	48	63
	C	18b	54	45	40	47
(Parked)	A	18c	45	48	40	44
	B	18c	55	70	56	60
	C	18c	43	49	42	44
0° TOE-OUT:						
Long Distance						
Taxi - Takeoff	B	19	76	82	83	80
(Airborne)						
Short Distance						
Taxi - Takeoff	B	20	51	48	47	49
(Airborne)						
Heavy Gross Weight						
Long Distance						
Taxi - Takeoff	B	21	97	106	100	101
(Airborne)						
Landing - Long						
Distance Taxi	B	22	63	79	80	73
(Parked)						
Landing - Short						
Distance Taxi	B	23	57	63	60	60
(Parked)						

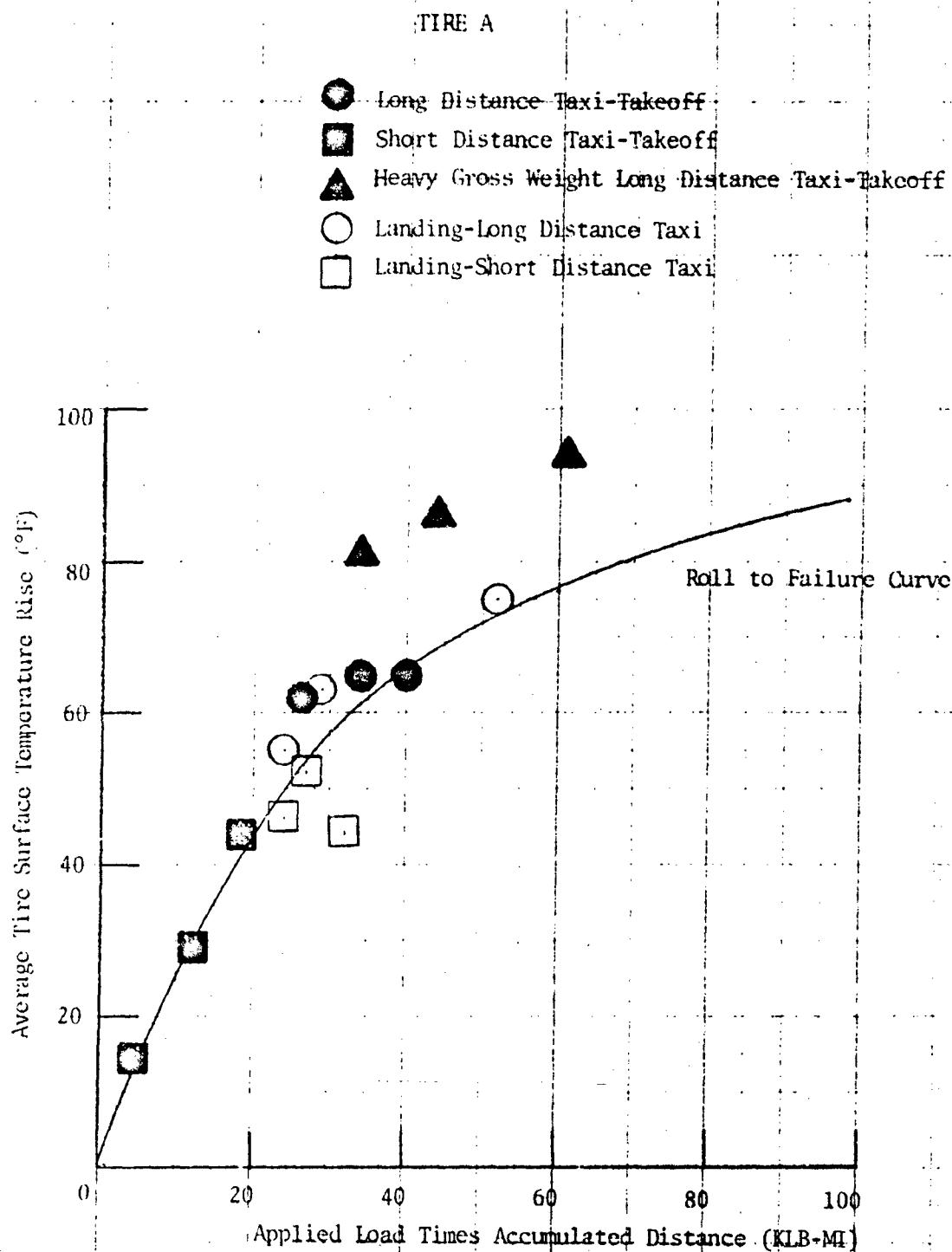


Figure 24. Average Tire Surface Temperature Rise Versus Applied Load Times Accumulated Distance for Laboratory Roll to Failure and Simulation Tests of Tire A

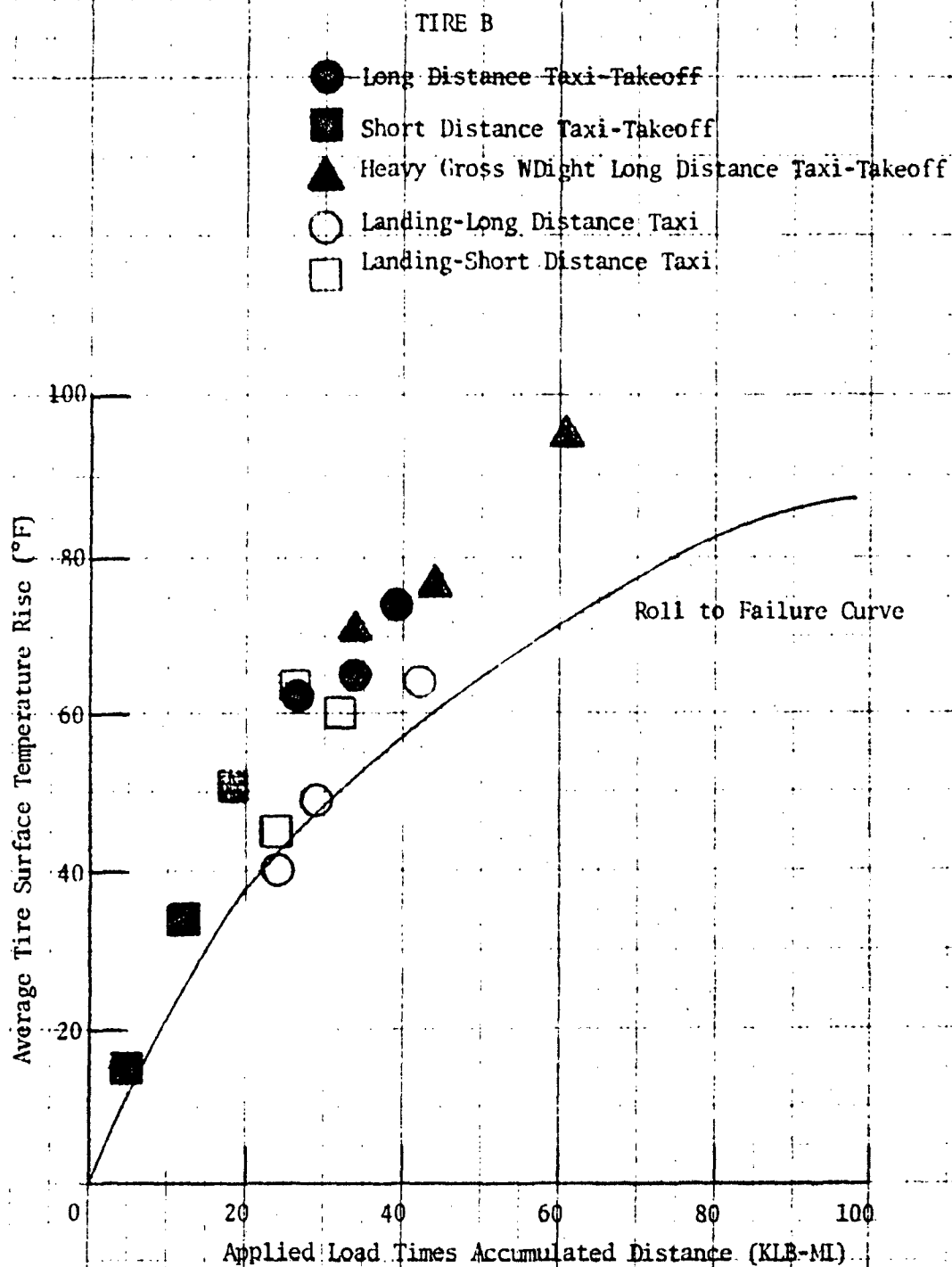


Figure 25. Average Tire Surface Temperature Rise Versus Applied Load Times Accumulated Distance for Laboratory Roll to Failure and Simulation Tests of Tire B

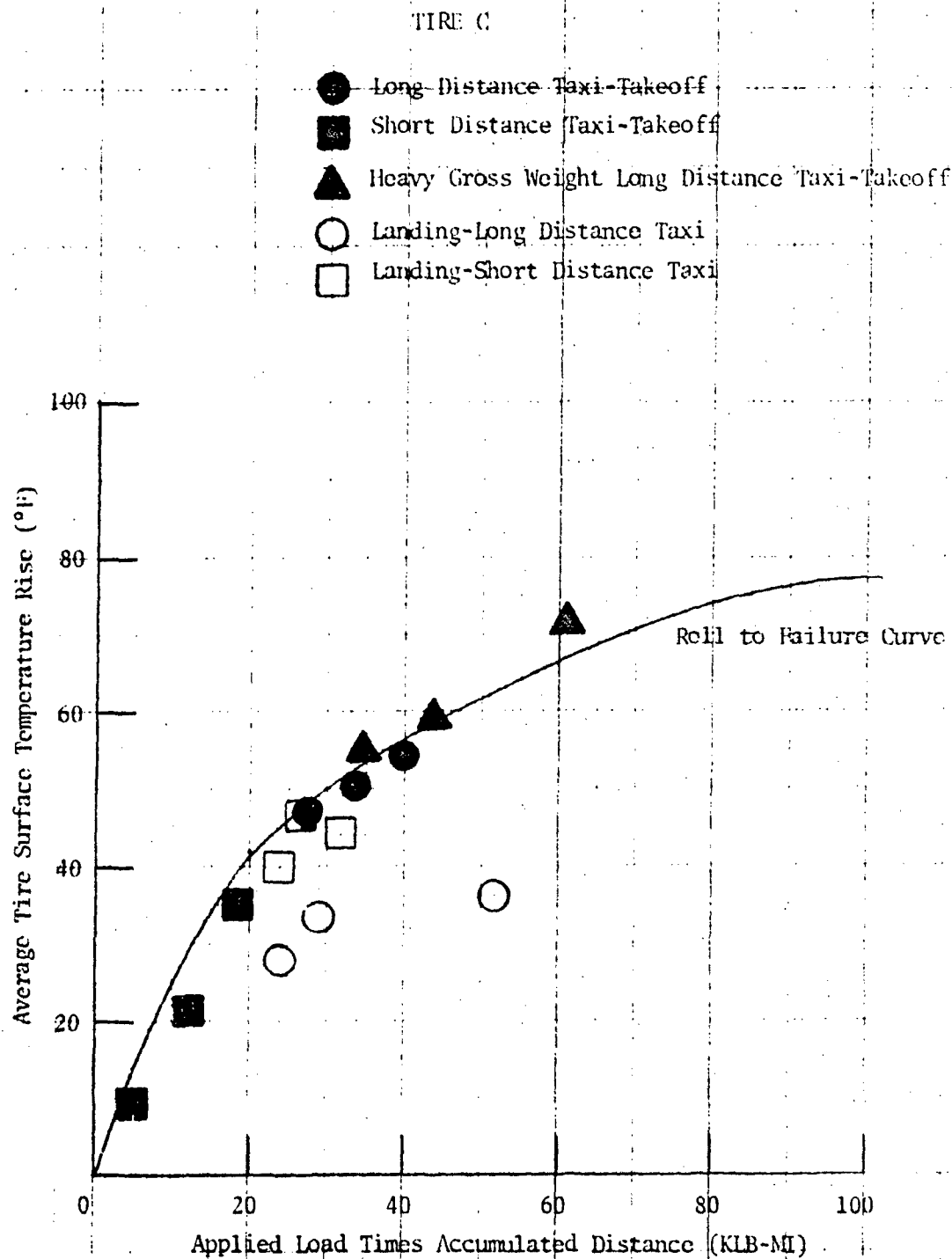


Figure 26. Average Tire Surface Temperature Rise Versus Applied Load Times Accumulated Distance for Laboratory Roll to Failure and Simulation Tests of Tire C.

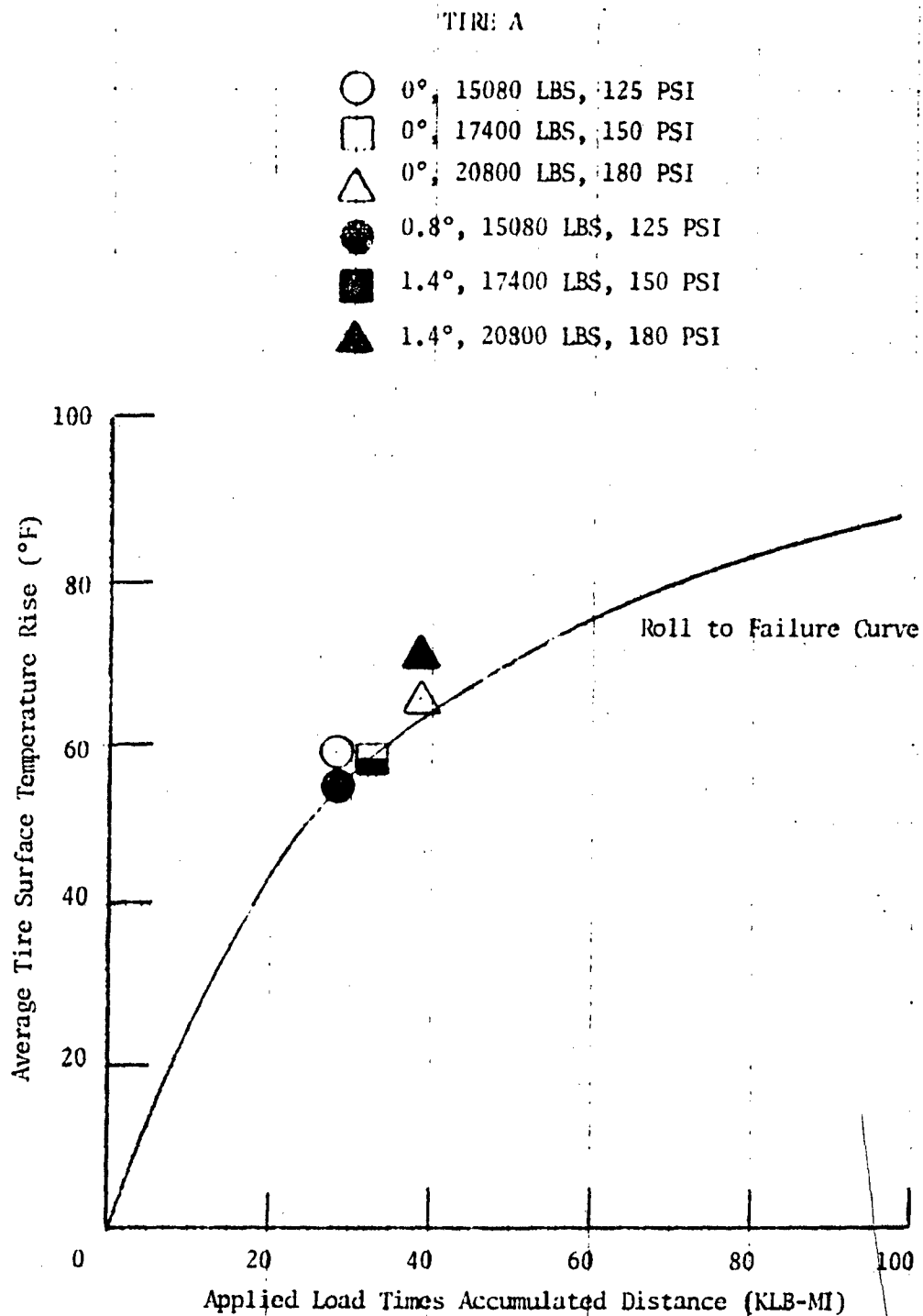


Figure 27. Average Tire Surface Temperature Rise Versus Applied Load Times Accumulated Distance Comparison Between Laboratory Roll to Failure Test and Taxi Tests for Tire A

(Figure 26). The taxi test surface temperature rise data were plotted with the roll to failure curve of Tire A in Figure 27.

The apparent discrepancy between the data of Figures 24, 25, and 26 which showed higher surface temperature rises for the laboratory simulation than for the roll to failure tests can be partially explained by the considerably different rates of heat generation existing between roll to failure and simulation tests. The choice of KLB-MI as the abscissa of these plots was made in an effort to correlate the diverse test conditions in terms of load and distance. To consider the added effect of the rate of heat generation requires the inclusion of a velocity contribution to the resultant temperature rise. As an example, the heavy gross weight long distance taxi-takeoff simulation required a total roll distance of 2.76 MI from leaving the chocks until airborne. The time required to achieve the total 60.72 KLB-MI was 11.6 minutes (see Appendix B). The corresponding time required to reach 60.72 KLB-MI or 3.04 MI, during the roll to failure test was 3.96 minutes. The corresponding average cyclic frequencies in achieving the 60.72 KLB-MI were 133 cycles/minute for the heavy gross weight simulation and 430 cycles/minute for the roll to failure test.

To illustrate the rate effects on tire surface temperatures, a plot of surface temperature rise divided by elapsed test time was constructed for Tire A (Figure 28). This plot clearly shows that all simulation tests had a rate of heat generation, as reflected by average tire surface temperature, that was well below the heat generation rate during the roll to failure tests. These data show that the magnitude of tire surface temperature was not by itself an indicator of incipient tire failure, but that the combined effects of load, distance and velocity must be considered in predicting tire failure. In an investigation of transport aircraft ground operations, Durup found that when taxiing equal distances at 10 MPH and 40 MPH, the higher speed will result in a 45% increase in tire bead temperature (Reference 4).

2. EFFECT OF SLIP ANGLE ON TIRE SURFACE TEMPERATURE

A comparison of the outboard and inboard sidewall temperature averages of Table 8 shows that when operating with a positive slip angle, the outboard sidewall ran consistently hotter than the inboard sidewall during the simulation and roll to failure tests. This conclusion was reinforced by conducting the simulation tests with 0 degree toe out which resulted in approximately equal

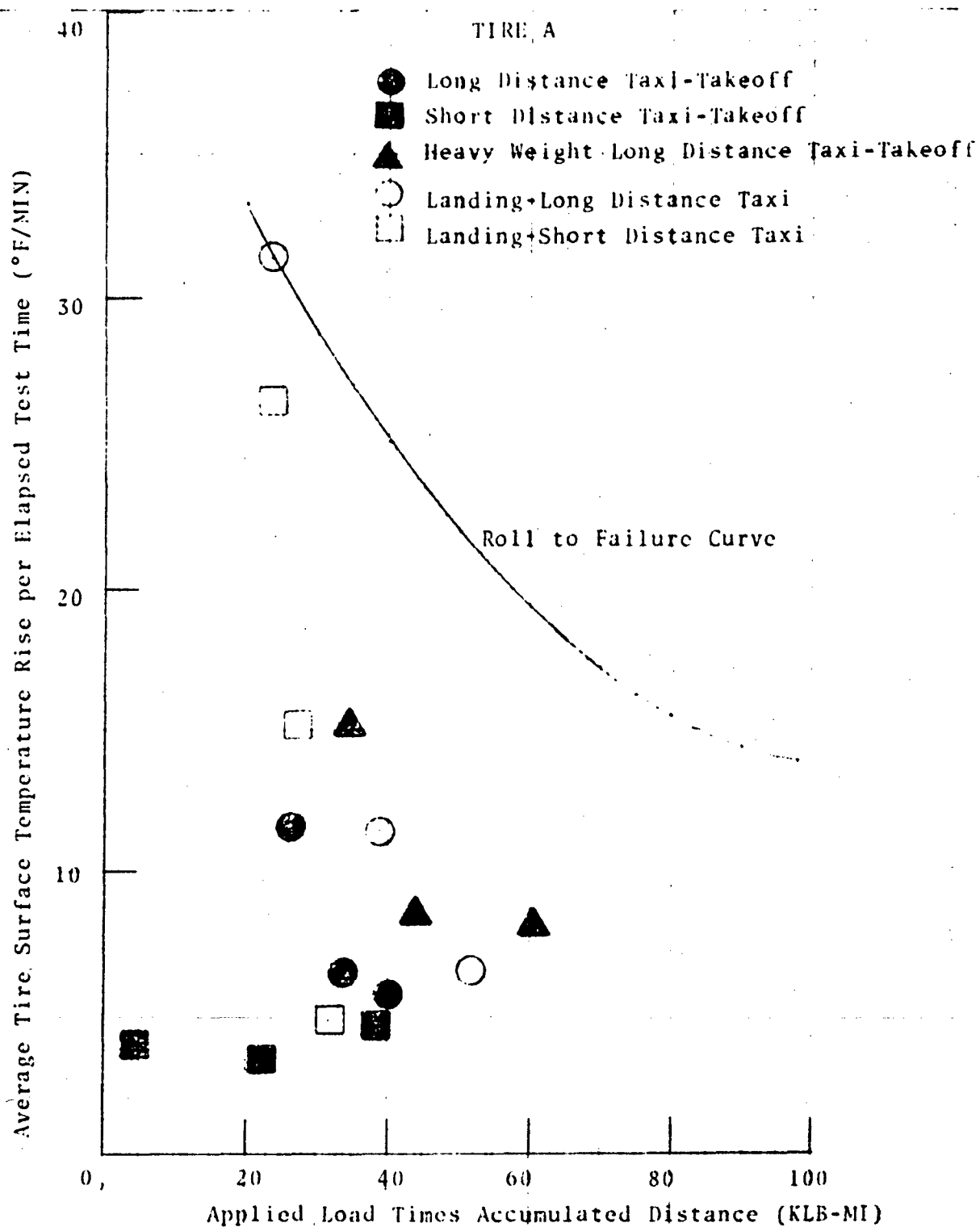


Figure 28. Average Tire Surface Temperature Rise per Elapsed Time Versus Applied Load Times Accumulated Distance for Laboratory Roll to Failure and Simulation Tests of Tire A

sidewall surface temperatures. The taxi test data from Table 8 does not correlate with the laboratory data with respect to the relationship between sidewall temperature difference and slip angle. These data show that the outboard sidewall temperature was higher than the inboard at both 0 degree and 1.4 degrees toe-out and was lower at the 0.8 degree toe-out. A possible explanation for these differences was the two right turns executed by the pilot: one right turn to enter the runway and another to leave the runway which occurred immediately prior to the sidewall measurements (Figure 9). Another possibility was that the gear had a torsional compliance that resulted in a toe-out equilibrium under rolling conditions.

3. OTHER INFLUENCES ON TIRE SURFACE TEMPERATURE

(a) Ambient, Runway and Flywheel Temperatures

At the start of each laboratory test involving surface temperature measurement, the tire and flywheel were at essentially ambient temperatures ranging from 69 to 87°F with an average ambient temperature for all laboratory tests of 77°F. No significant effect on tire surface temperatures was apparent from these different ambient temperatures.

During the taxi tests at Edwards AFB, the ambient temperatures ranged from 68 to 97°F, while the concrete runway temperatures were 74 to 111°F. Since these tests required coordination of runway usage with other aircraft, the tires were often not in equilibrium but only relatively close to ambient at the start of the test. For example, Figure 11, second section, shows an initial average temperature of 121°F which indicates that the tire had some heat content prior to the test since the average ambient and runway temperatures for these two runs were 93 and 102°F. To obtain a correlation between ambient, runway and tire surface temperatures would require the conduction of the same test with the same tire over a relatively wide range of temperatures.

(b) Speed

The effect of speed as related to the rate of heat generation has already been discussed. The effect of increased speed on tire surface temperature measurement has been noted (3) as having a cooling effect on the surface

due to the increased air flow over the tire. During the laboratory simulation and taxi tests, the surface temperature measurements were taken with the tire stopped. During the roll to failure tests, the measurements were taken with the tire rolling at a constant 46 MPH, and would therefore exhibit slightly lower surface temperatures than if the tire were stopped.

(c) Circumferential Temperature Variation

The temperatures in this report were obtained using the line scan method of thermography and represent the temperatures along a meridional line extending from bead to bead. Since a tire, by virtue of its less than perfect construction, has circumferential temperature variations; temperature differences can be obtained for the same tire. When the tire is rolling, circumferential variations can be averaged during the measurement. When the tire is stopped, the measurement may yield temperatures that are somewhat higher or lower than the average circumferential temperature. Surface irregularities, such as embossed or indented lettering on the tire sidewall, will create slightly higher or lower surface temperatures due to the small increase or decrease of section at the lettering. These small irregularity induced temperature differences were not considered to be true circumferential temperature variations.

SECTION VI

CONCLUSIONS

1. The simulation tests resulted in laboratory tire failures that were in agreement with field failure data for the small sample of tires that were tested.
2. Imminent aircraft tire failure cannot be predicted by the measurement of surface temperature alone.
3. Operating a tire with small positive slip angles resulted in consistently higher outboard (versus inboard) sidewall temperatures. The magnitude of the difference between sidewall surface temperatures (outboard minus inboard) appeared to be a linear function of small slip angles.
4. No tire tread surface temperature gradient as a result of operating with small slip angles was noted in either laboratory or field testing.
5. The 24 ply rate tire, Tire C, ran considerably cooler than either of the 22 ply rated Tires A or B

SECTION VII

RECOMMENDATIONS

1. The laboratory simulation that was developed for the A-10 was based on actual airfield ground operations. This type of simulation should be used where realistic ground loading spectra are required.
2. Infrared thermography, since it is relatively easy to use, should be used in tire tests so that a body of data on various sizes of tires can be accumulated, analyzed, and correlated.
3. Infrared thermography should prove to be a valuable adjunct to the measurement methods presently employed during full scale laboratory brake tests. Full field thermographs of the tire, wheel, piston housing, and portions of the pressure plate and backing plate could be studied to identify heat flow paths, temperature gradients, and hot spots. Any regions of excessively high temperatures, as identified by the thermograph, could be further instrumented to gather additional data. This combination of thermography and thermocouples would be a thermal measurement analogy to the practice of using brittle coatings and strain gages that has proved successful in experimental stress analysis.

APPENDIX A

**CARPET PLOT OF CORNERING FORCE VERSUS NORMAL
LOAD, INFLATION PRESSURE AND SMALL SLIP ANGLES**

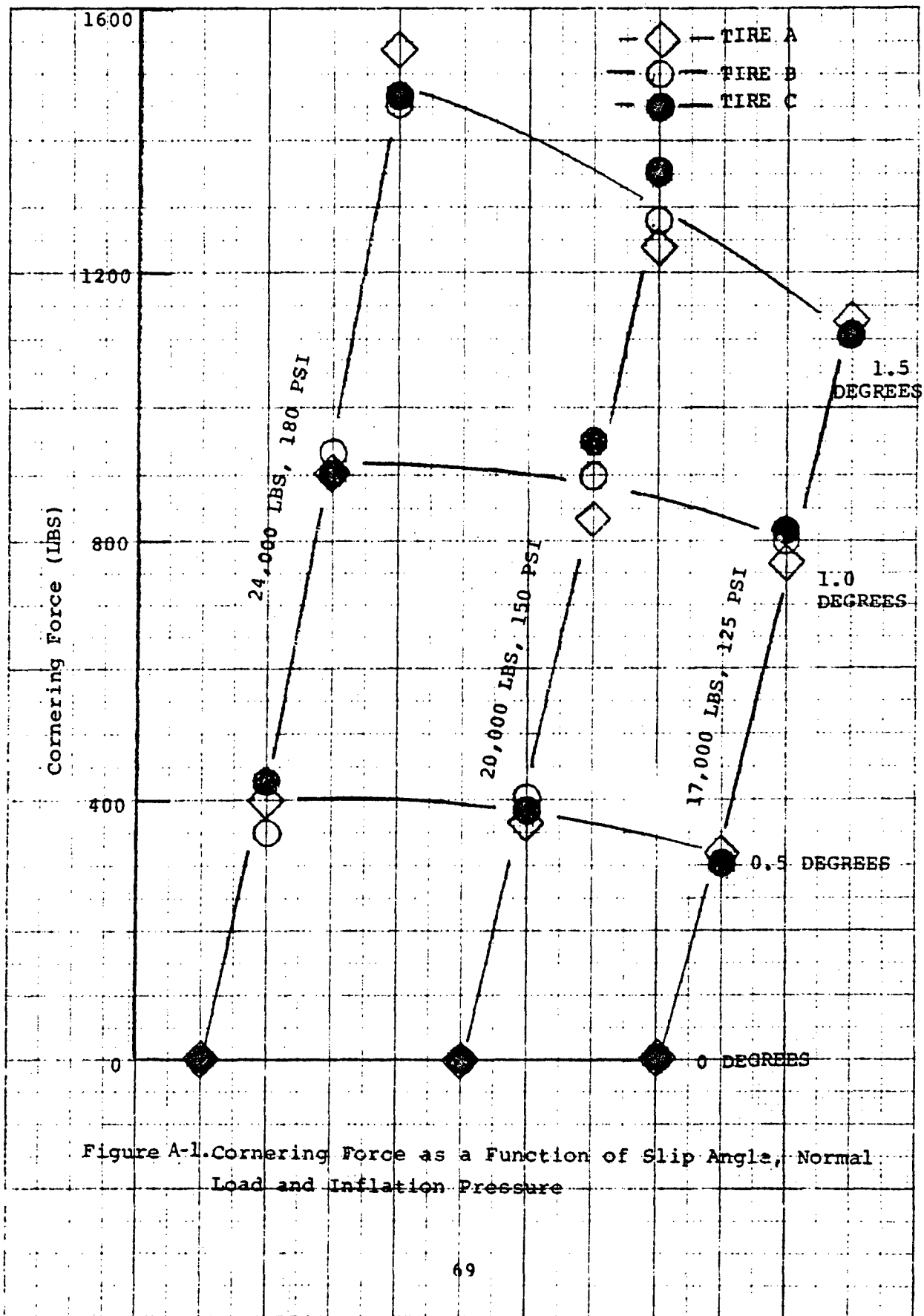


Figure A-1. Cornering Force as a Function of Slip Angle, Normal Load and Inflation Pressure

APPENDIX B

**DETAILED DYNAMICS STATEMENTS FOR THE MYRTLE
BEACH SIMULATION**

Condition 1 - Long Distance Taxi/Take-off

Unless otherwise specified, the tire will operate with a -0.8° yaw angle. Measure the flat-plate deflection at 19,000 lb radial load and 150 psi inflation pressure. Set deflection on the dynamometer by maintaining 150 psi inflation and reducing the radial load.

	<u>Time</u>	<u>Distance</u>
1. Load tire on flywheel	0	0
2. Accelerate from 0 to 5 mph in 5 seconds	5	18
3. Roll 30 ft at 5 mph in 4 seconds	9	48
4. Make a 90° left turn in 8 seconds at 5 mph using a 1.3° yaw angle	17	103
5. Roll 800 ft at 5 mph in 109 seconds	126	903
6. Make a 90° left turn in 8 seconds at 5 mph using a 1.3° yaw angle	134	958
7. Accelerate from 5 mph to 30 mph in 10 seconds	144	1215
8. Roll 6686 ft at 30 mph for 152 seconds	296	7901
9. Decelerate from 30 mph to 5 mph in 10 seconds	306	8158
10. Make a 90° left turn in 8 seconds at 5 mph using a 1.3° yaw angle	314	8213
11. Decelerate from 5 mph to 0 in 5 seconds	319	8231
12. Stop for 120 seconds	439	8231
13. Accelerate from 0 to 5 mph in 5 seconds	444	8249
14. Make a 90° right turn in 8 seconds at 5 mph using a -2.9° yaw angle	452	8304
15. Roll 150 ft at 5 mph for 20 seconds	472	8454
16. Make a 90° right turn in 8 seconds at 5 MPH using a -2.9° yaw angle	480	8509
17. Roll 80 ft at 5 mph for 11 seconds	491	8589
18. Make a 90° left turn in 8 seconds at 5 mph using a 1.3° yaw angle	499	8644

19. Accelerate from 5 mph to 20 mph in 10 seconds	509	8327
20. Roll 150 ft at 20 mph for 5 seconds	514	8977
21. Decelerate from 20 mph to 15 mph in 5 seconds	519	9105
22. Make a 90° right turn in 14 seconds at 15 mph using a -2.5° yaw angle	533	9419
23. Roll 800 ft at 15 mph for 36 seconds	569	10219
24. Decelerate from 15 mph to 5 mph in 5 seconds	574	10292
25. Make a 90° right turn in 8 seconds at 5 mph using a -2.9° yaw angle	582	10347
26. Roll 110 ft at 5 mph for 15 seconds	597	10457
27. Decelerate from 5 mph to 0 in 10 seconds	607	10494
28. Stop for 60 seconds	667	10494

(End of taxi)

29. Program the dynamometer for a take-off as specified by the following load and velocity versus time table.

<u>Time (Sec)</u>	<u>Velocity (MPH)</u>	<u>Radial Load (Lb)</u>
0	0	W*
5	45	
10	85	
15	120	
18	141	0.96 W
18.2	143	0 W

*W is the load required to reach flat plate deflection.

End of Test.

Condition 2 - Short Distance Taxi/Take-off

Unless otherwise specified, the tire will operate with a -0.8° yaw angle. Measure the flat-plate deflection at 19,000 lb radial load and 150 psi inflation pressure. Set deflection on the dynamometer by maintaining 150 psi inflation and reducing the radial load.

	<u>Time</u>	<u>Distance</u>
1. Load tire on flywheel	0	0
2. Accelerate from 0 to 5 mph in 5 seconds	5	18
3. Roll 30 ft at 5 mph in 4 seconds	9	48
4. Make a 90° left turn in 8 seconds at 5 mph using a 1.3° yaw angle	17	103
5. Roll 800 ft at 5 mph in 109 seconds	126	903
6. Make a 90° right turn in 8 seconds at 5 mph using a -2.9° yaw angle	134	958
7. Roll 520 ft at 5 mph in 71 seconds	205	1478
8. Make a 90° right turn in 8 seconds at 5 mph using a -2.9° yaw angle	213	1533
9. Decelerate from 5 mph to 0 in 5 seconds	218	1551
10. Stop for 120 seconds	338	1551
11. Accelerate from 0 to 5 mph in 5 seconds	343	1569
12. Make a 90° left turn in 8 seconds at 5 mph using a 1.3° yaw angle	351	1624
13. Roll 150 ft at 5 mph for 20 seconds	371	1774
14. Make a 90° left turn in 8 seconds at 5 mph using a 1.3° yaw angle	379	1829
15. Roll 80 ft at 5 mph for 11 seconds	390	1909
16. Make a 90° right turn in 8 seconds at 5 mph using a -2.9° yaw angle	398	1964
17. Accelerate from 5 mph to 15 mph in 5 seconds	403	2056
18. Roll 428 ft at 15 mph for 19 seconds	422	2056

19. Make a 90° left turn in 14 seconds at 15 mph using a 2.1° yaw angle	436	3798
20. Roll 800 ft at 15 mph for 36 seconds	472	3598
21. Decelerate from 15 mph to 5 mph in 5 seconds	477	3671
22. Make a 90° left turn in 8 seconds at 5 mph using a 2.1° yaw angle	485	3726
23. Roll 110 ft at 5 mph for 15 seconds	500	3830
24. Decelerate from 5 mph to 0 in 10 seconds	510	3873
25. Stop for 60 seconds	570	3873

(End of taxi)

26. Program the dynamometer for a take-off as specified in Condition 1.

Condition 3 - Maximum Gross Weight, Long Distance Taxi/Take-off

Unless otherwise specified, the tire will operate with a -0.8° yaw angle. Measure the flat-plate deflection at 24,000 lb radial load and 180 psi inflation pressure. Set deflection on the dynamometer by maintaining 180 psi inflation and reducing the radial load.

	<u>Time</u>	<u>Distance</u>
1. Load tire on flywheel	0	0
2. Accelerate from 0 to 5 mph in 5 seconds	5	18
3. Roll 30 ft at 5 mph in 4 seconds	9	48
4. Make a 90° left turn in 8 seconds at 5 mph using a 1.3° yaw angle	17	103
5. Roll 800 ft at 5 mph in 109 seconds	126	903
6. Make a 90° left turn in 8 seconds at 5 mph using a 1.3° yaw angle	134	958
7. Accelerate from 5 mph to 30 mph in 10 seconds	144	1215
8. Roll 6686 ft at 30 mph for 152 seconds	296	7901
9. Decelerate from 30 mph to 5 mph in 10 seconds	306	8158
10. Make a 90° left turn in 8 seconds at 5 mph using a 1.3° yaw angle	314	8213
11. Decelerate from 5 mph to 0 in 5 seconds	319	8231
12. Stop for 120 seconds	439	8231
13. Accelerate from 0 to 5 mph in 5 seconds	444	8249
14. Make a 90° right turn in 8 seconds at 5 mph using a -2.9° yaw angle	452	8304
15. Roll 150 ft at 5 mph for 20 seconds	472	8454
16. Make a 90° right turn in 3 seconds at 5 MPH using a -2.9° yaw angle	480	8509
17. Roll 30 ft at 5 mph for 11 seconds	491	8589
18. Make a 90° left turn in 3 seconds at 5 mph using a 1.3° yaw angle	499	8644

Accelerate from 5 mph to 20 mph in 10 seconds	509	3827
Roll 150 ft at 20 mph for 5 seconds	514	8977
Decelerate from 20 mph to 15 mph in 5 seconds	519	9105
Make a 90° right turn in 14 seconds at 15 mph using a -2.5° yaw angle	533	9419
Roll 300 ft at 15 mph for 36 seconds	569	10219
Decelerate from 15 mph to 5 mph in 5 seconds	574	10292
Make a 90° right turn in 8 seconds at 5 mph using a -2.9° yaw angle	582	10347
Roll 110 ft at 5 mph for 15 seconds	597	10457
Decelerate from 5 mph to 0 in 10 seconds	607	10494
Stop for 60 seconds	667	10494

(End of taxi)

1. Program the dynamometer for a take-off as specified by the following load and velocity versus time table.

<u>Time (Sec)</u>	<u>Velocity (MPH)</u>	<u>Radial Load (Lb)</u>
0	0	W*
27	157	0.98W
29.5	188	0

*W is the load required to reach flat plate deflection.

End of test.

Condition 4 - Landing/Long Distance Taxi

Unless otherwise specified, the tire will operate with a -0.8° yaw angle. Measure the flat-plate deflection at 15,000 lb radial load and 150 psi inflation. Set deflection on the dynamometer by maintaining 150 psi inflation and reducing the radial load.

1. Land against flywheel rotating with a peripheral speed of 150 mph, apply load and decelerate as shown in the following table:

Accumulations

			<u>Time (Sec)</u>	<u>Distance (Ft)</u>
<u>Time (Sec)</u>	<u>Velocity (MPH)</u>	<u>Radial Load (Lb)</u>		
0	150	0	0	0
6	125	1.1 W*	6	1760
28	70	W	28	4500
105	5	W	105	9000
*W is the load required to reach flat plate deflection.				
2. Make a 90° left turn in 8 seconds at 5 mph using a 1.3° yaw angle			113	9055
3. Accelerate from 5 mph to 15 mph in 5 seconds			118	9147
4. Roll 800 ft at 15 mph for 36 seconds			154	9947
5. Make a 90° left turn in 15 seconds at 15 mph using a 2.1° yaw angle			168	10261
6. Accelerate from 15 mph to 20 mph in 5 seconds			173	10389
7. Roll 150 ft at 20 mph for 5 seconds			178	10539
8. Decelerate from 20 mph to 5 mph in 10 seconds			188	10722
9. Make a 90° right turn in 8 seconds at 5 mph using a -2.9° yaw angle			196	10777
10. Roll 80 ft at 5 mph for 11 seconds			207	10857
11. Decelerate from 5 mph to 0 in 5 seconds			212	10875

12. Stop for 120 seconds	332	10875
13. Accelerate from 0 to 5 mph in 5 seconds	337	10930
14. Make a 90° left turn in 8 seconds at 5 mph using a 1.3° yaw angle	345	10985
15. Roll 150 ft at 5 mph for 20 seconds	365	11135
16. Make a 90° left turn in 8 seconds at 5 mph using a 1.3° yaw angle	373	11190
17. Roll 80 ft at 5 mph for 11 seconds	384	11270
18. Make a 90° right turn in 8 seconds at 5 mph using a -2.9° yaw angle	392	11325
19. Accelerate from 5 mph to 30 mph in 10 seconds	402	11582
20. Roll 6686 ft at 30 mph for 152 seconds	554	18268
21. Decelerate from 30 mph to 5 mph in 10 seconds	564	18525
22. Make a 90° right turn in 8 seconds at 5 mph using a -2.9° yaw angle	572	18580
23. Roll 800 ft at 5 mph in 109 seconds	681	19380
24. Make a 90° right turn in 8 seconds at 5 mph using a -2.9° yaw angle	689	19435
25. Decelerate from 5 mph to 0 in 5 seconds	694	19453

End of Test

Condition 5 - Landing/Short Distance Taxi

Unless otherwise specified, the tire will operate with a -0.8° yaw angle. Measure the flat-plate deflection of 15,000 lb radial load and 150 psi inflation. Set deflection on the dynamometer by maintaining 150 psi inflation and reducing the radial load.

1. Land against flywheel rotating with a peripheral speed of 150 mph, apply load and decelerate as shown in the following table:

Accumulations

Time (Sec) Distance (Ft)

<u>Time (Sec)</u>	<u>Velocity (MPH)</u>	<u>Radial Load (Lb)</u>
0	150	0
6	125	1.1 W*
28	70	W
105	10	W

0	0
6	1760
28	4500
105	9000

*W is the load required to be at flat-plate deflection.

2. Make a 90° right turn in 16 seconds at 10 mph using a -1.5° yaw angle.	121	9235
3. Roll 680 ft at 10 mph for 46 seconds	167	9915
4. Make a 90° right turn in 21 seconds at 10 mph using a -1.5° yaw angle	188	10223
5. Decelerate from 10 mph to 5 mph in 5 seconds.	193	10277
6. Make a 90° left turn in 8 seconds at 5 mph using a 1.3° yaw angle.	201	10332
7. Decelerate from 5 mph to 0 in 5 seconds	206	10350
8. Stop for 120 seconds	326	10350
9. Accelerate from 0 to 5 mph in 5 seconds	331	10368
10. Make a 90° right turn in 8 seconds at 5 mph using a -2.9° yaw angle	339	10423
11. Roll 150 ft at 5 mph for 20 seconds	359	10573
12. Make a 90° right turn in 8 seconds at 5 mph using a -2.9° yaw angle.	367	10628

13. Roll 80 ft at 5 mph for 11 seconds	378	10708
14. Make a 90° left turn in 8 seconds at 5 mph using a 1.3° yaw angle.	386	10763
15. Roll 400 ft at 5 mph for 55 seconds	441	11163
16. Make a 90° left turn in 8 seconds at 5 mph using a 1.3° yaw angle	449	11218
17. Roll 300 ft at 5 mph in 109 seconds	558	12018

End of test.

APPENDIX C

CONTAINED AIR TEMPERATURE AND PRESSURE DURING THE SIMULATION TESTS

TABLE C-1.
CONTAINED AIR TEMPERATURE
AND PRESSURE FROM THE
LABORATORY SIMULATION TESTS*

<u>CONDITION</u>	<u>TIRE I.D.</u>	<u>TEMPERATURE (°F)</u>		<u>PRESSURE (PSI)</u>	
		<u>INITIAL</u>	<u>FINAL</u>	<u>INITIAL</u>	<u>FINAL</u>
1	A	79	144	150	174
	B	69	143	150	174
	C	77	131	150	171
2	A	78	122	150	162
	B	75	126	150	162
	C	81	116	150	161
3	A	73	167	180	216
	B	85	180	180	213
	C	75	147	180	212
4	A	73	148	150	175
	B	87	151	150	176
	C	80	116	150	172
5	A	76	120	150	170
	B	71	131	150	169
	C	75	119	150	165

These data represent the average of ten test runs.

REFERENCES

1. N. M. Trivisonno, "Thermal Analysis of a Rolling Tire." SAE Paper 700474, May, 1970.
2. N. M. Trivisonno, "Non-Steady-State Thermal Analysis of a Rolling Aircraft Tire." SAE Paper 720871, October, 1972.
3. F. S. Conant, G. L. Hall, and J. D. Walter, "Surface Temperature of Running Tires Using Infrared Scanning." SAE Paper 700475, May, 1970.
4. P. C. Durup, "Improvement of Overload Capability of Air Carrier Aircraft Tires." DOT Report FAA RD-78-133, October, 1978.

BIBLIOGRAPHY

Tire Temperature

Conant, F. S., "Tire Temperatures." RUBBER CHEMISTRY and TECHNOLOGY, 44, (2), 397 (1971).

Perhaps the most comprehensive publication dealing with tire temperatures and their measurement.

Rolling Resistance and Power Loss

Skele, Peters, "Rolling Resistance and Carcass Life of Tires Operating at High Deflections." AFFDL-TR-70-138, February, 1972.

Bogden, L., and Rice, R. S., "Laboratory and Full-Scale Parametric Studies of the Rolling Resistance of Radial-and-Bias-Ply Heavy Service Truck Tires." DOT-HS-805-690, November, 1980.

Tire temperature, power loss and rolling resistance are all interdependent.

Aircraft Braking Effects on Tire Temperature

Brookman, B. J., "Transient Thermal Effects in Disc Brakes." AFFDL-TR-79-3112, November, 1979.

Perhaps the most definitive work on the analytical prediction of landing gear component temperatures achieved by aircraft braking.